Neutral meson production measured with the ALICE experiment

Adam Matyja

on behalf of the ALICE Collaboration

Institute of Nuclear Physics PAN, Cracow, Poland

- Motivation
- ALICE detector
- Neutral mesons in pp, p-Pb and Pb-Pb
  - Production spectra
  - η/π^0 ratio and m_T scaling
  - Nuclear modification factor R_{AA} and Q_{pA}
- Summary

Motivation

- Explore Quantum Chromodynamics (QCD) in unknown regimes → study QCD phase diagram
- Investigate properties of nuclear matter at high temperature ($T \geq 170$ MeV or 2×10^{12} K) and density
- Important input for the understanding of the chiral symmetry restoration and the deconfinement (transition from hadronic to quark matter)
- Quark Gluon Plasma (QGP) phase produced < 10^{-6} s after the Big Bang
- Search for QGP phase and measure its properties
- LHC gives us the great opportunity via heavy ion collisions ("little Big Bangs")

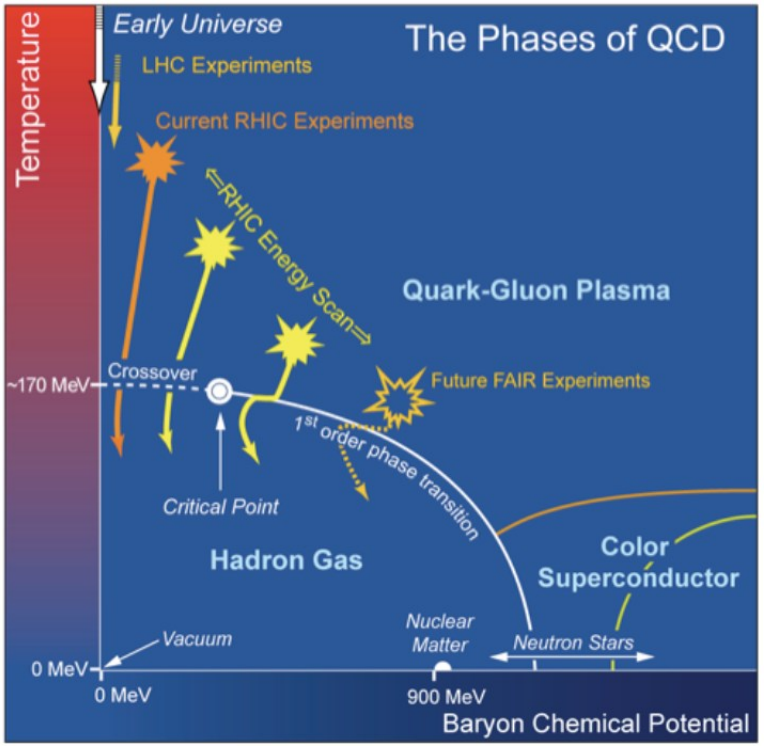

Why neutral mesons?

- Meson production in pp at large transverse momentum is described by pQCD
- Neutral meson spectra allow to put constraints on parameters of theoretical models in both perturbative (NLO, NNLO) and non-perturbative regime (parton distribution function, fragmentation function)
- Hadrons carry information about medium
  - Studies of transport properties or initial gluon density of quark-gluon matter
  - Quark/gluon energy loss difference
- Test scaling laws
- Disentangle initial/final state effects
- Neutral mesons are major background source for direct photon and dielectron analyses

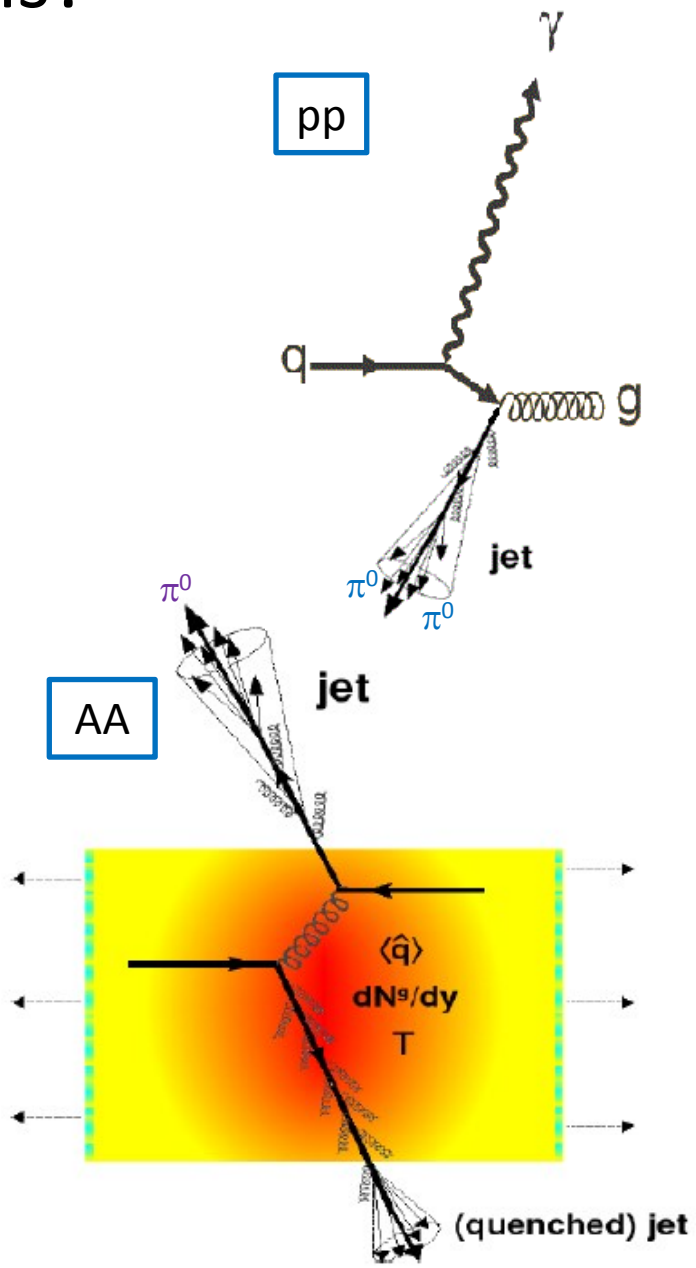

ALICE detector

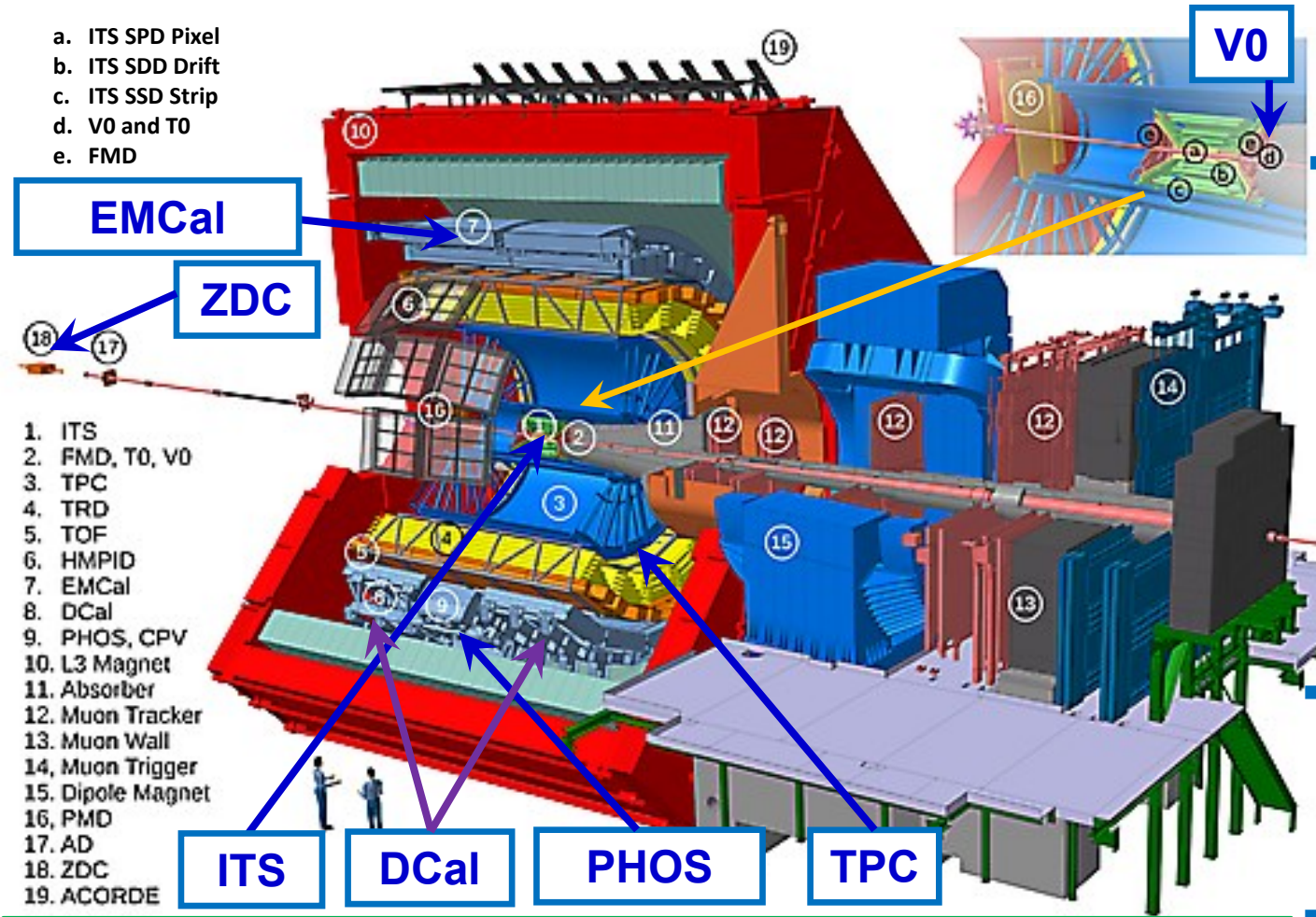

- Tracking ($e^{\pm}$, $h^{\pm}$)
  - PCM (γ, π^0, η)
  - $|\eta| < 0.9$, $0 < \varphi < 2\pi$
  - TPC - gas drift detector
  - ITS - silicon detector
- EMCal + DCal (γ, π^0, η)
  - Pb-scintillator sampling calorimeter
  - Trigger
  - $|\eta| < 0.7$, $80^o < \varphi < 187^o$
  - $0.22 < |\eta| < 0.7$, $260° < \varphi < 320°$,
  - $|\eta| < 0.7$, $320^o < \varphi < 327^o$
- PHOS (γ, π^0, η)
  - $PbWO_4$ crystal spectrometer
  - Trigger
  - $|\eta| < 0.13$, $260^o < \varphi < 320^o$
- Vertex
  - Pixel
- V0 and ZDC
  - Centrality determination
  - Trigger

Neutral mesons

Invariant mass

$$M_{\gamma\gamma} = \sqrt{2E_1E_2(1-\cos\theta_{12})}$$

pp @ 0.9 , 7 TeV:	PLB 717(2012) 162-172.
pp @ 2.76 TeV:	EPJC 74 (2014) 3108; EPJC 77 (2017) 339.
pp @ 8 TeV:	EPJC 78 (2018) 263.
p-Pb @ 5.02 TeV:	EPJC 78 (2018) 624 .
Pb-Pb @ 2.76 TeV:	EPJC 74 (2014) 3108; PRC98 (2018) 044901.

Tracking System = ITS + TPC

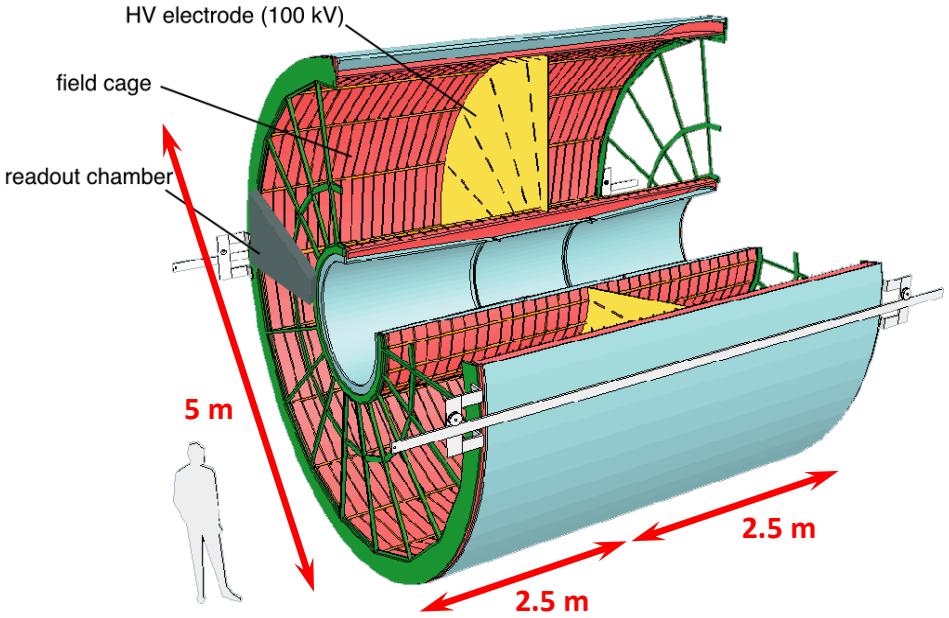

TPC – time projection chamber

- Diameter × Length : 5 m × 5 m
- Acceptance: $\Delta\varphi = 2\pi$, $|\eta| < 0.9$
- Readout chambers: 72
- Pad readout (3 types): 557 568
- Drift field: 400 V/cm
- Maximum drift time: 92 μs
- Central electrode HV: 100 kV
- Gas:
  - Active volume: 90 m^3
  - Ne-CO_2-N_2: 85.7% - 9.5% - 4.8%

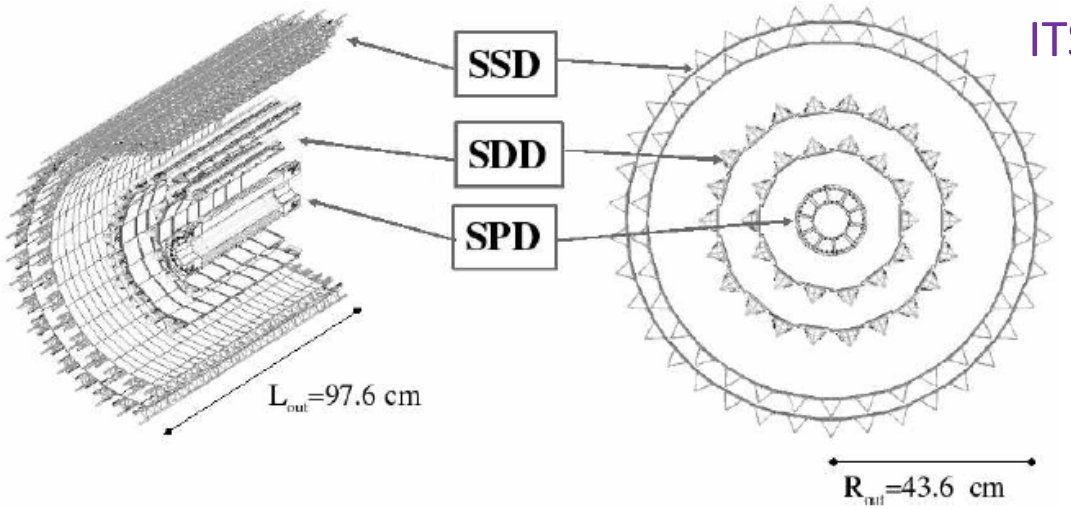

ITS – inner tracking system

- Layout
  - 2 layers of pixel detectors
  - 2 layers of drift detectors
  - 2 layers of strip detectors
- Acceptance: $\Delta\varphi = 2\pi$, $|\eta| < 0.9$

Calorimeters

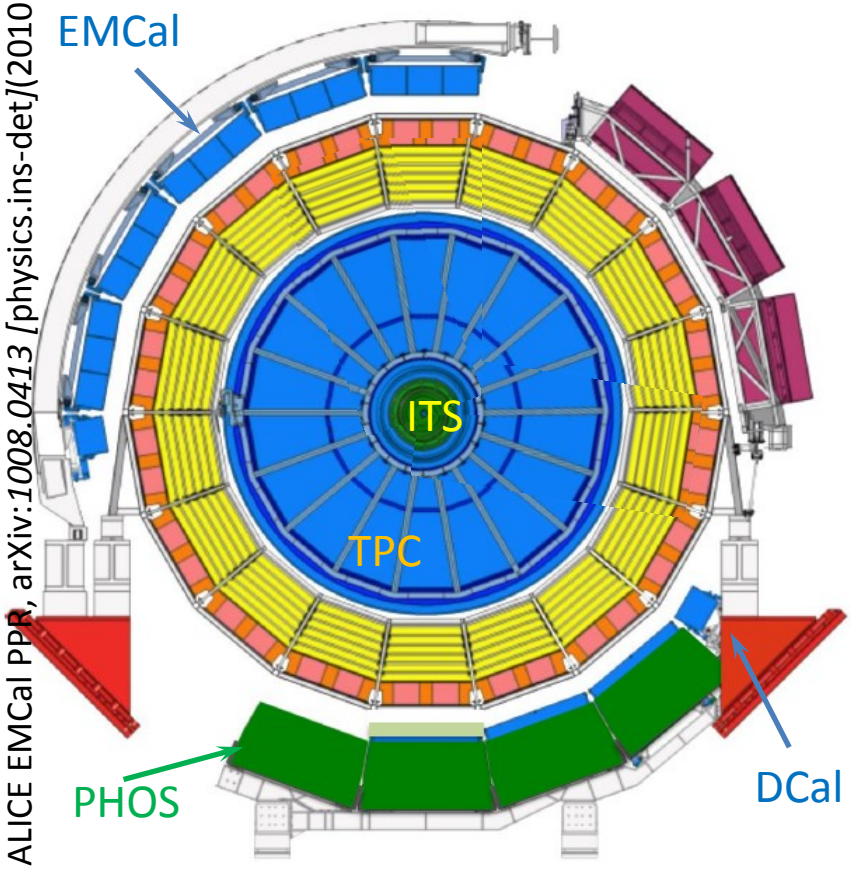

ALICE EMCal PPR, arXiv:*1008.0413 [*physics.ins-det*]*(2010).

EMCal + DCal - electromagnetic calorimeter

- Lead (76 layers) scintillator (77 layers) shashlik
- Tower size: 6 cm × 6 cm × 24.6 cm
- 20 super-modules (10 + 4 × 1/3 + 6 × 2/3)
- Acceptance: 80° < φ < 187°, $|\eta| < 0.7$ (EMCal)
- Acceptance: 260° < φ < 320°, $0.22 < |\eta| < 0.7$ (DCal)
- Acceptance: 320° < φ < 327°, $|\eta| < 0.7$ (DCal)
- 428 cm from the beam line
- ~ 20 radiation length
- Energy resolution:
  $\sigma/E = (4.8 \pm 0.8)/E \oplus (11.3 \pm 0.5)/\sqrt{E} \oplus (1.7 \pm 0.3)\%.$

PHOS – photon spectrometer

- Crystal of lead tungstate ($PbWO_4$)
- 3.5 × 64 × 56 crystals of size: 2.2 × 2.2 × 18 cm^3
- Acceptance: 250° < φ < 320°, $|\eta| < 0.13$
- Energy resolution: $\sigma/E = 1.3/E \oplus 3.6/\sqrt{E} \oplus 1.12\ \%$
- Distance to IP: 4.6 m

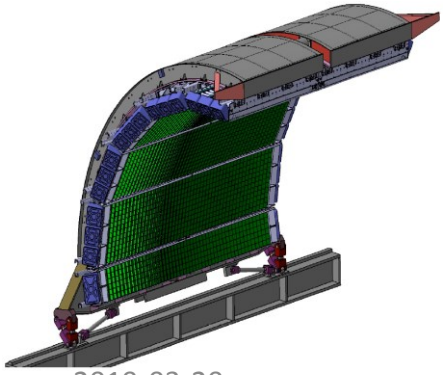

EMCal Module

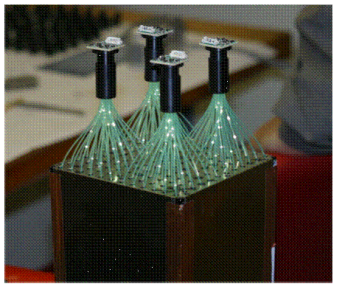

PHOS crystal

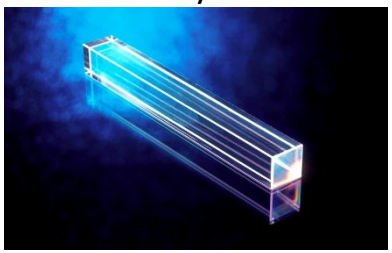

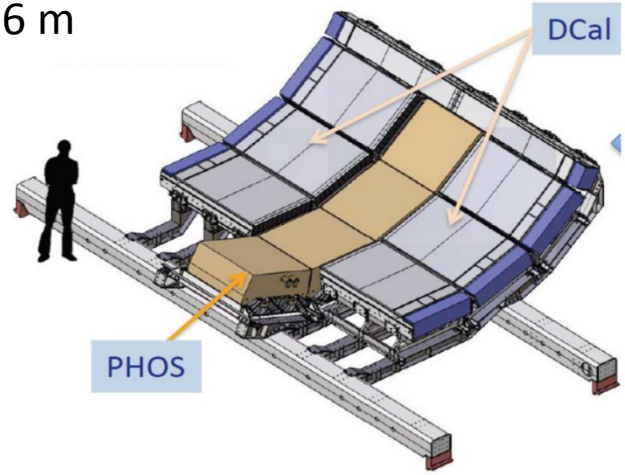

Method of neutral meson extraction

- Invariant mass analysis:

→ photon pairs or external conversion electrons

  - $h \rightarrow \gamma + \gamma$ (PHOS, EMCal)
  - $h \rightarrow \gamma (\rightarrow e^+ e^-) + \gamma (\rightarrow e^+ e^-)$ (PCM)
    - Small conversion probability (~ 8.5 %) is compensated by a wide acceptance.
  - Dalitz decays $h \rightarrow \gamma \gamma^* \rightarrow \gamma (\rightarrow e^+ e^-) e^+ e^-$
  - Hybrid methods (PHOS + PCM, EMCal +PCM)

- Shower shape
  - High p_T π^0 decay pairs - showers overlap

Distribution of conversions

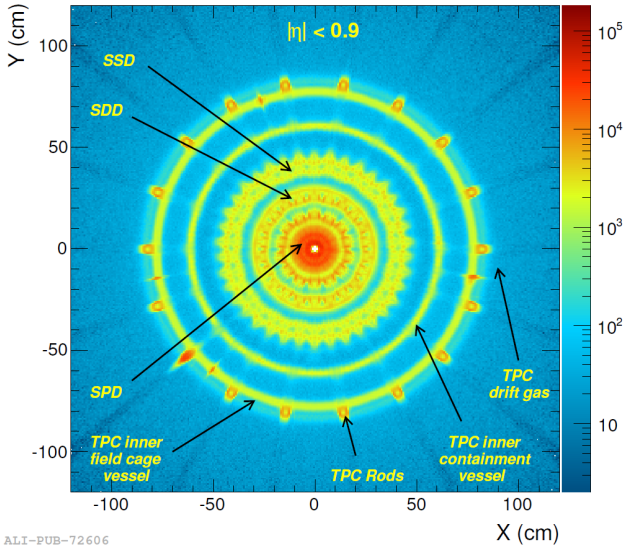

Int. J. Mod. Phys. A **29**, 1430044 (2014)

Material budget well known with relative precision of 4.5 %.
Radiation length $X/X_0 = (11.4 \pm 0.5)$ %.

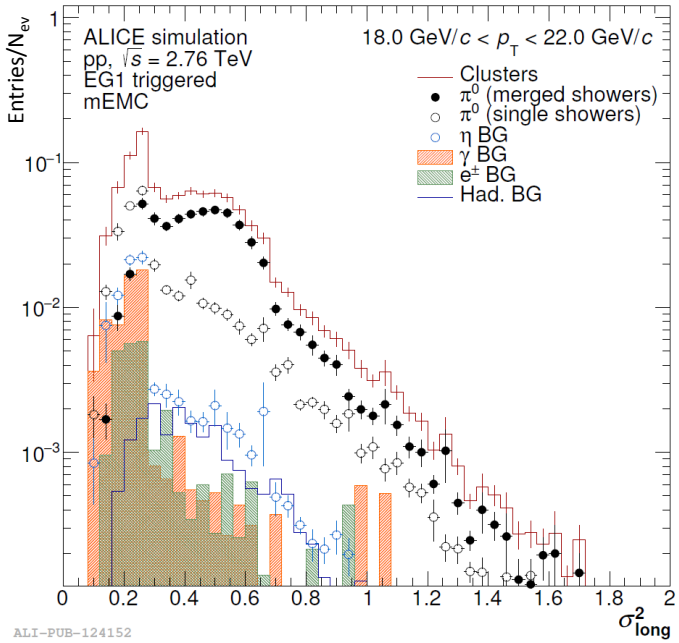

EPJC 77 (2017) 339

$$\sigma^2_{long} = 0.5\left(\sigma^2_{\varphi\varphi} + \sigma^2_{\eta\eta} + \sqrt{(\sigma^2_{\varphi\varphi} - \sigma^2_{\eta\eta})^2 + 4\sigma^4_{\eta\varphi}}\right),$$

$$\sigma^2_{\alpha\beta} = <\alpha\beta> - <\alpha><\beta>,$$

$$<\alpha> = \frac{\sum w_i \alpha_i}{\sum w_i},$$

Neutral meson reconstruction

- Invariant mass $M_{\gamma\gamma} = \sqrt{2E_1E_2(1-\cos\theta_{12})}$
- Event mixing to estimate combinatorial background
- Extraction of signal (exponent + Gaussian) and background (polynomial) parameterization
- Corrections based on MC
- Merging results from different methods

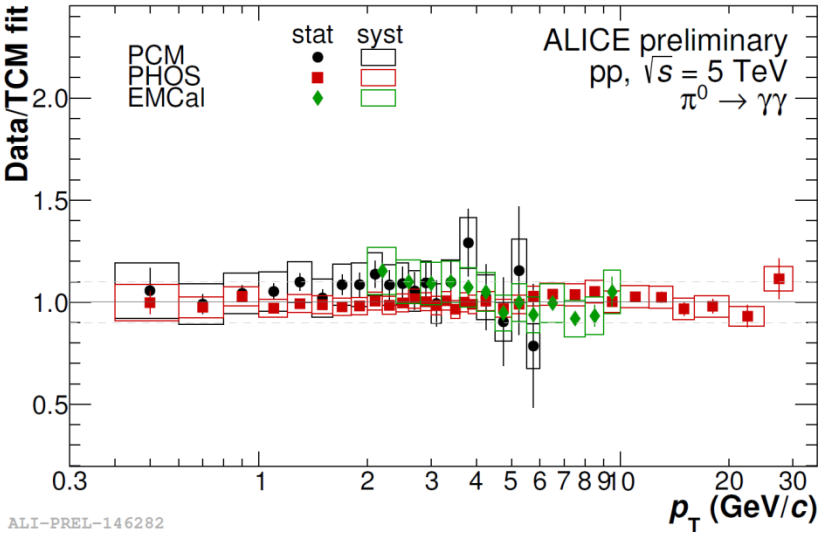

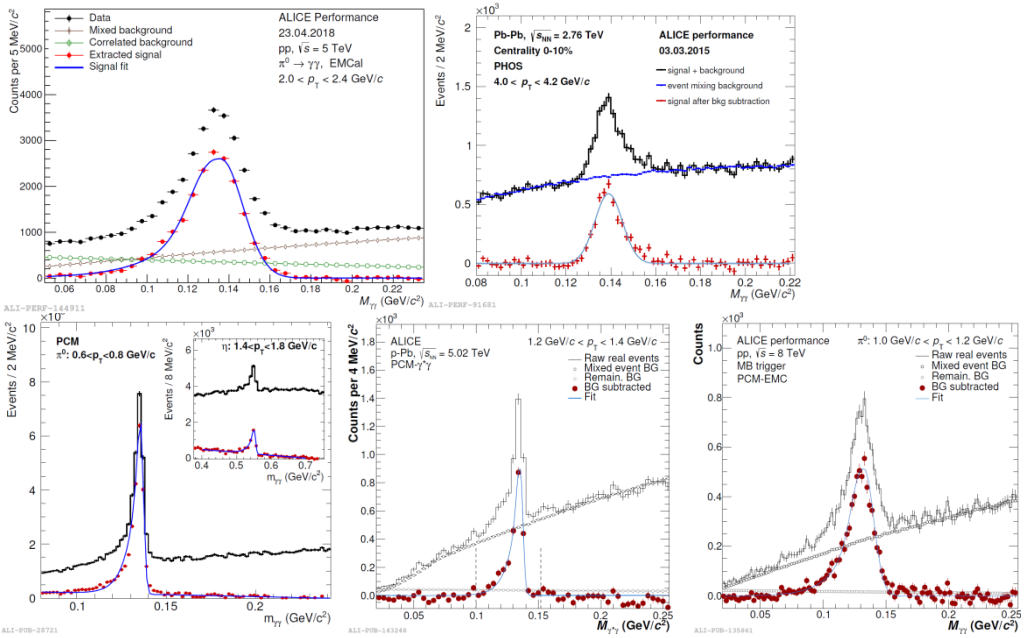

$$E\frac{\mathrm{d}^3\sigma}{\mathrm{d}p^3} = \frac{N_{\mathrm{rec}}}{p_{\mathrm{T}}^{*}\,\Delta p_{\mathrm{T}}\,\varepsilon\,\varepsilon_{\mathrm{trig}}}\,\frac{1}{L_{\mathrm{int}}}\,\frac{1}{\mathrm{BR}}$$

Neutral mesons are reconstructed

- For different collision energies
- In different systems (pp, p-Pb, Pb-Pb)
- Via different methods (detectors)
- In wide p_T range

Good agreement between methods allowed for combined result

Neutral meson spectra in pp

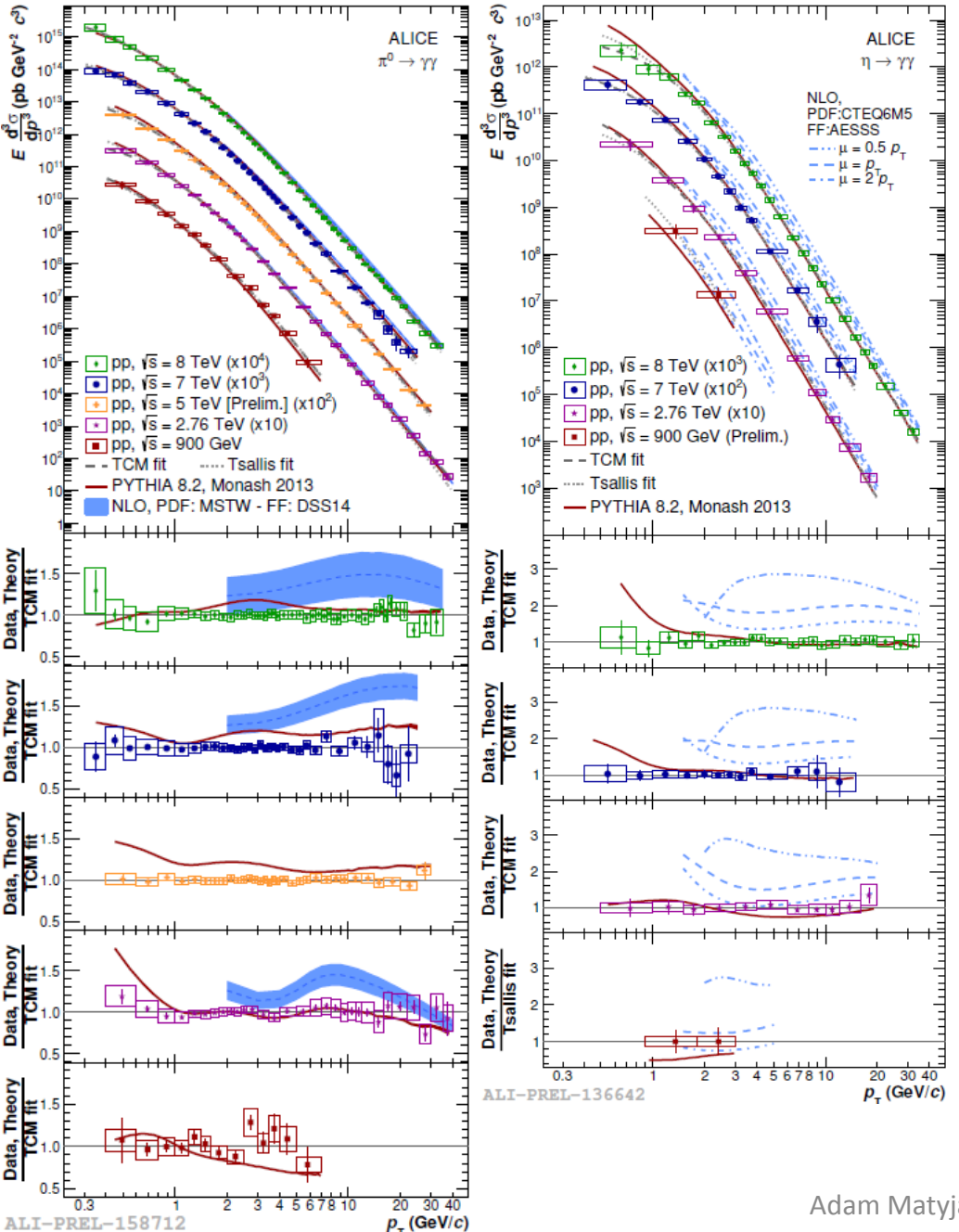

- Preliminary result of π^0 spectrum for energy $\sqrt{s}$ = 5 TeV
- π^0 and η mesons reconstructed in wide p_T range
- Power law dependence at high p_T
- PYTHIA 8.2 Monash 2013 MC describes data, but shows a bump at mid-p_T for higher energies
- NLO calculations overpredict data for both π^0 (20% - 60%) and η (50% - 100%)
  - Update on η FF is desired (as done for pions and kaon)

0.9 , 7 TeV: PLB 717(2012) 162-172.
2.76 TeV: EPJC 74 (2014) 3108; EPJC 77 (2017) 339.
8 TeV: EPJC 78 (2018) 263

NLO: PRD 91 (2015) 1, 014035

Meson production in p-Pb at $\sqrt{s_{NN}}$ = 5.02 TeV

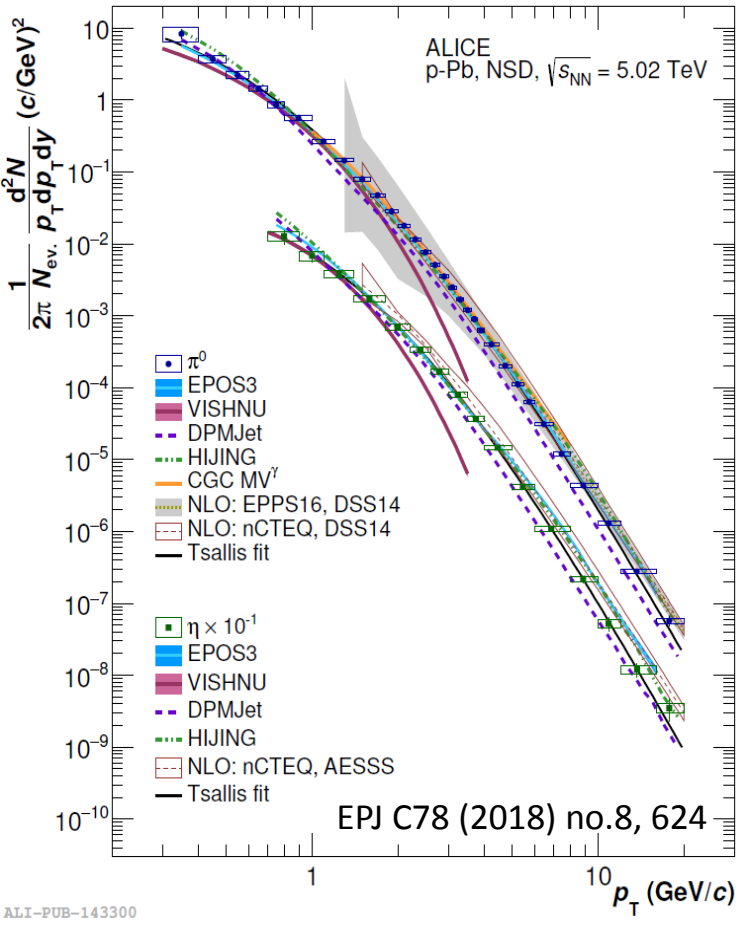

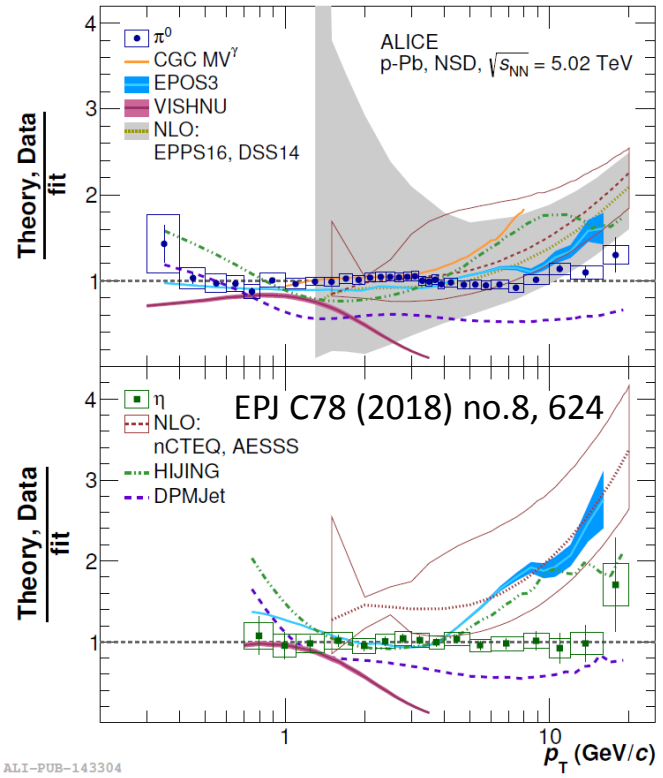

Wide p_T range:

- $0.3 < p_T < 20$ GeV/c (π^0)
- $0.7 < p_T < 20$ GeV/c (η)

- Data described by Tsallis function
- EPOS3 model describes π^0 spectrum (expected)
  - η spectrum reproduced for $p_T < 4$ GeV/c
- VISHNU (hydro) model describes low-p_T range (expected)
- Good description of π^0 spectrum by NLO pQCD calculations, but fails for η in high-p_T region

EPOS3: K.Werner et al., PRC89 (2014) 064903.
VISHNU: C.Shen at al., PRC95 (2017) 014906.
CGC: T.Lappi et al., PRD88 (2013) 114020.

Meson production in centrality classes in p-Pb at $\sqrt{s_{NN}}$ = 5.02 TeV

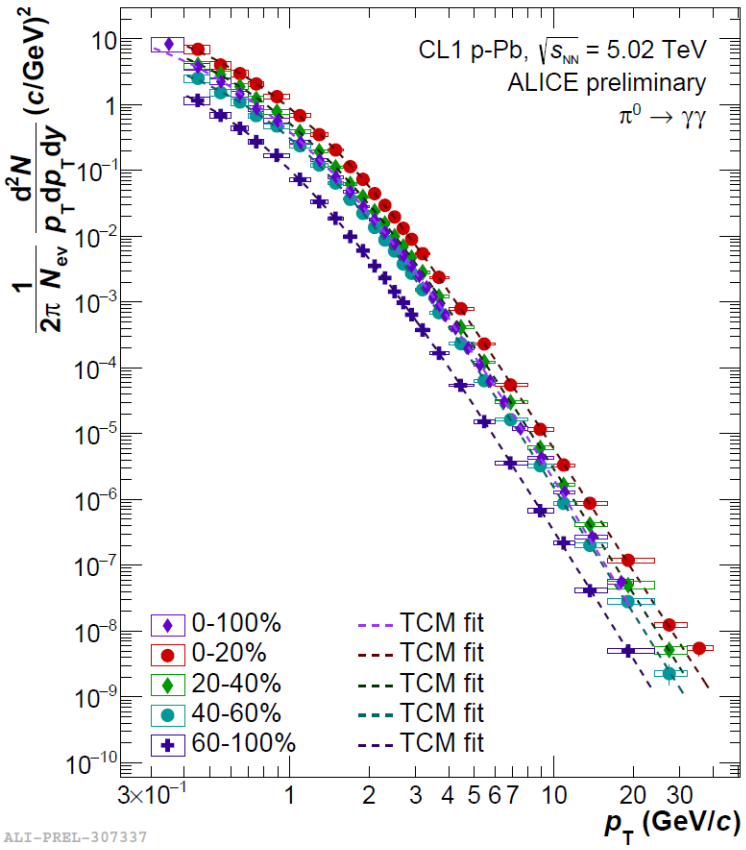

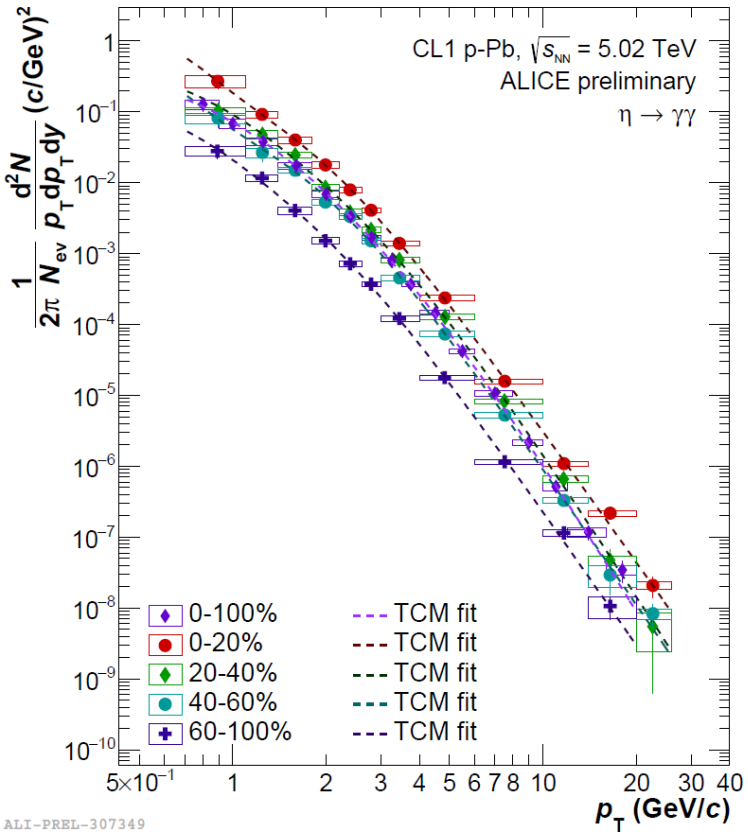

NSD p-Pb0-100%:
EPJ C78 (2018) 624

- Spectra of π^0 and η mesons measured in 4 centrality classes
- Extended p_T range $\rightarrow$ up to 40 GeV/c by using PHOS trigger

Model comparisons

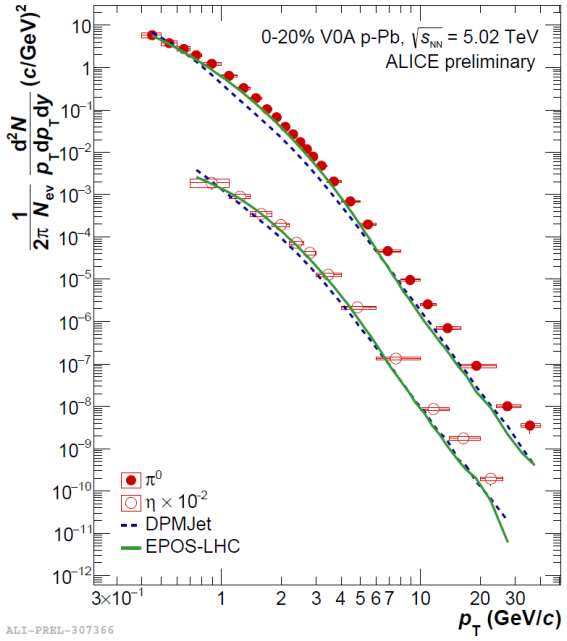

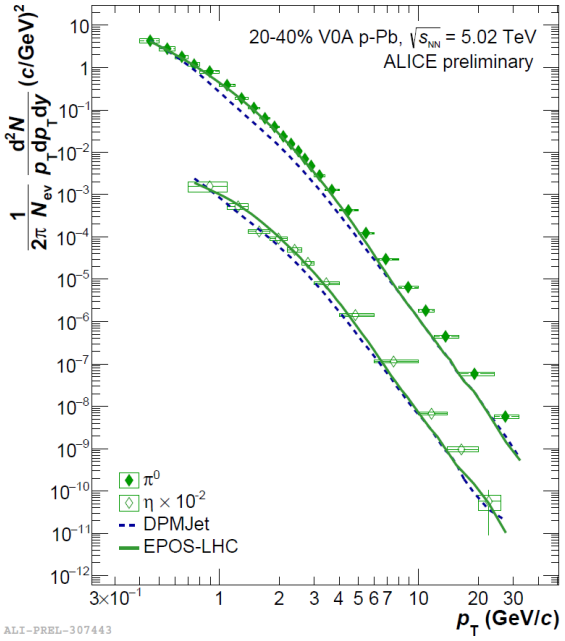

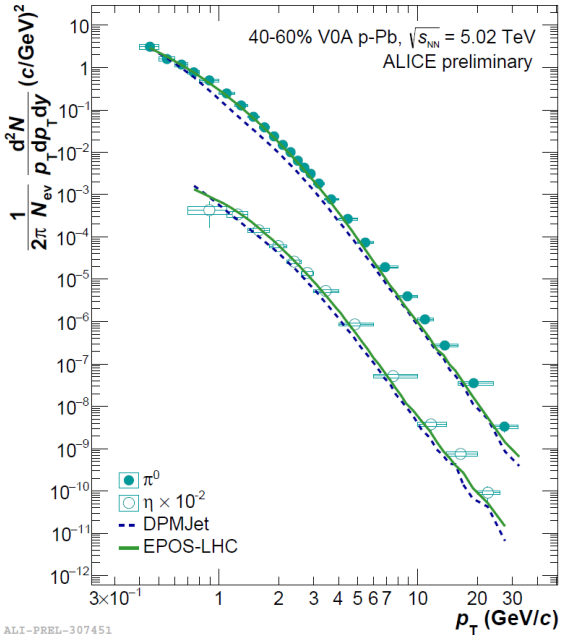

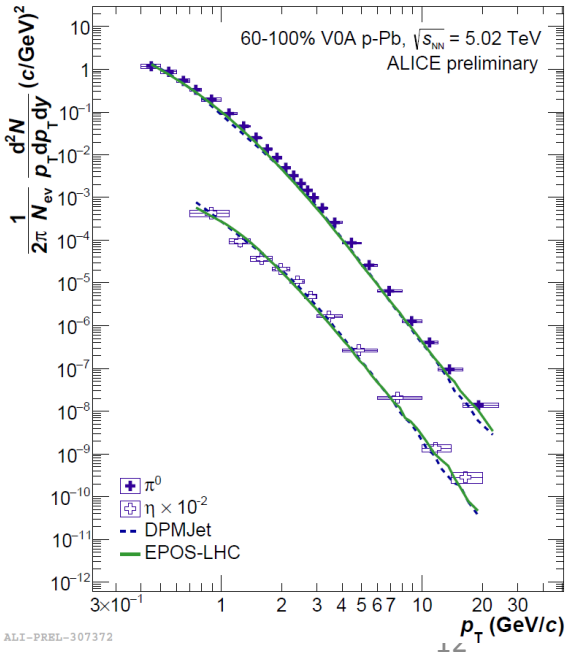

- Both DPMJet and EPOS-LHC underpredict data at high p_T for every centrality class
- Low p_T data better described by EPOS-LHC than DPMJet

Neutral meson spectra in Pb-Pb at $\sqrt{s_{NN}}$ = 2.76 and 5.02 TeV

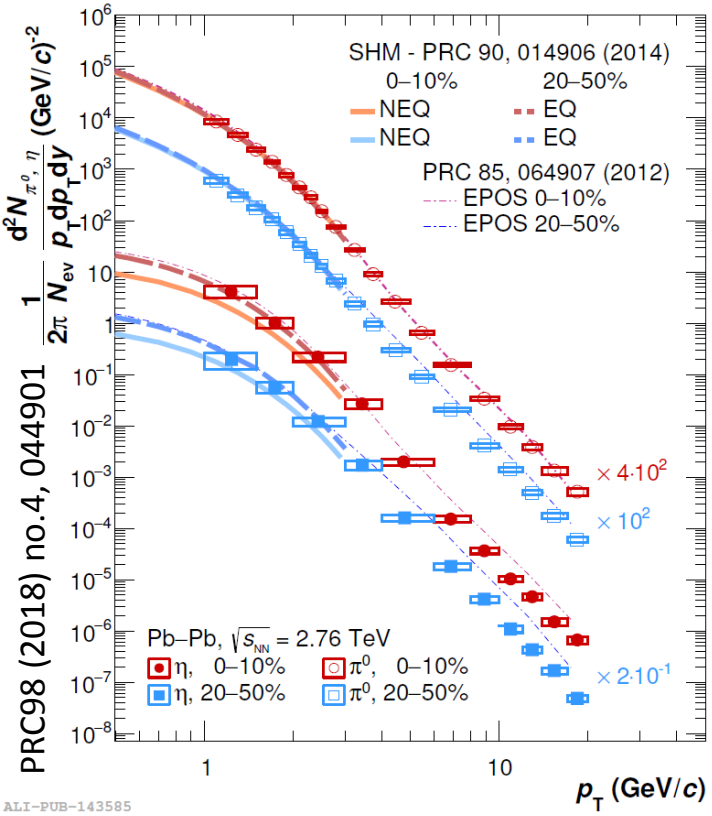

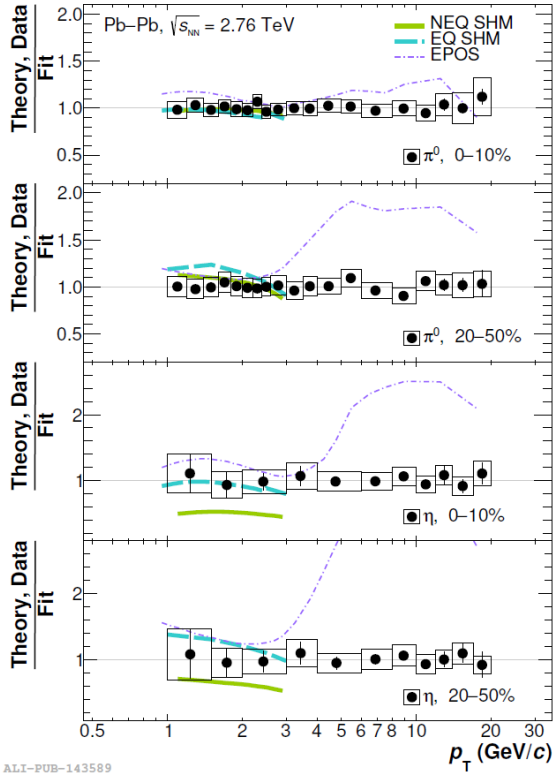

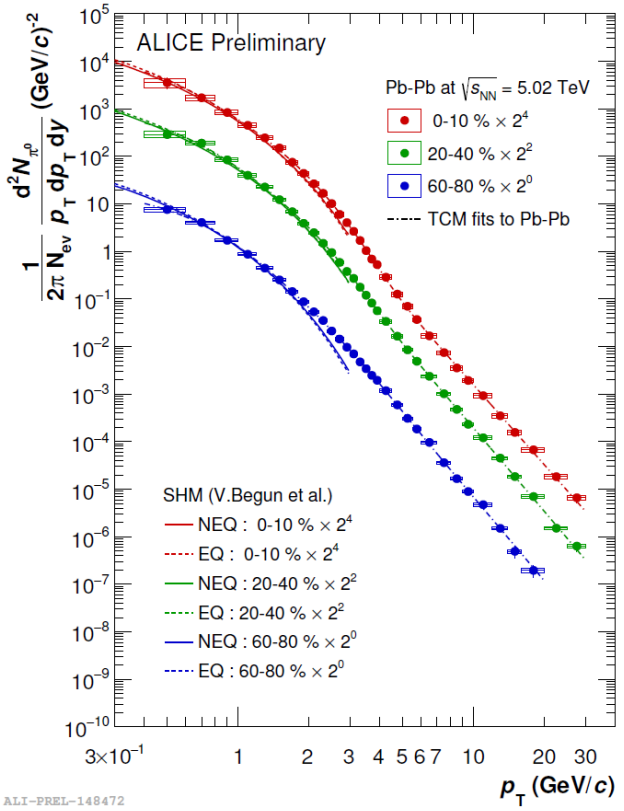

- Extended range up to p_T = 20 GeV/c for π^0 at $\sqrt{s_{NN}}$ = 2.76 TeV in comparison to PLB 717 (2012) 162-172
- First measurement of the η meson in Pb-Pb collisions at the LHC
- Preliminary measurement of π^0 spectrum in several centrality classes at $\sqrt{s_{NN}}$ = 5.02 TeV in the range $0.4 < p_T < 30$ GeV/c
- Good description of low-p_T region, failure or no description of high-p_T range

η/π^0 ratio and m_T scaling

EPJC 78 (2018) 263

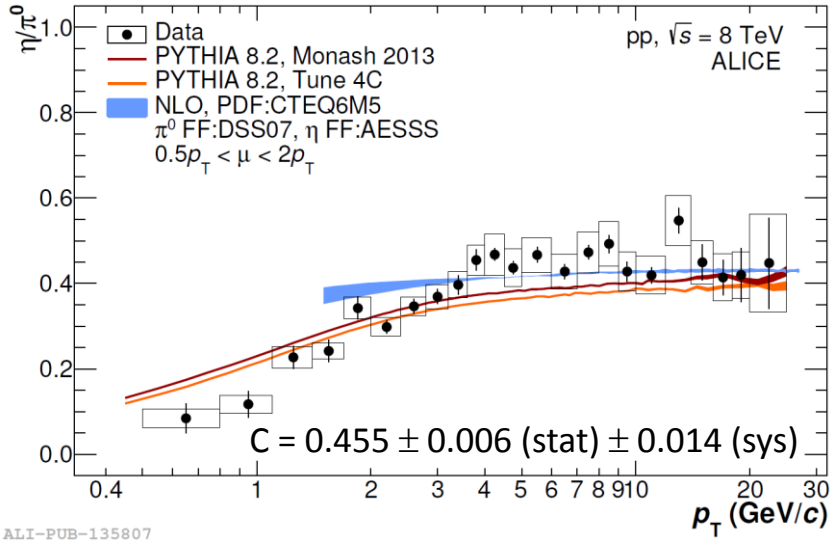

EPJC 77 (2017) 5,339

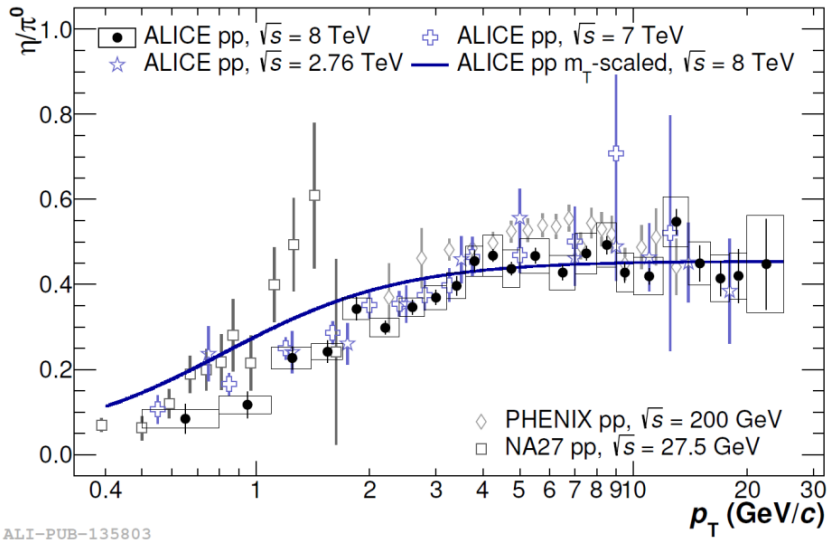

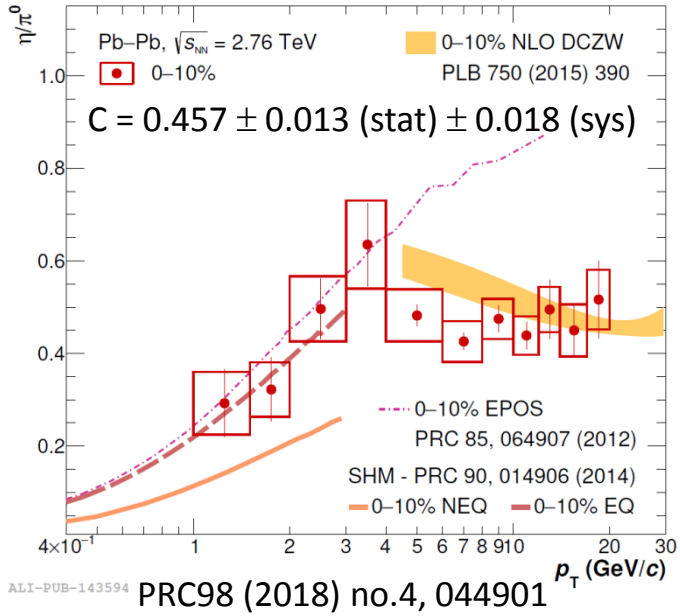

PRC98 (2018) no.4, 044901

- $E\,d^3\sigma/dp^3 = C^m f(m_T)$
- Universal η/π^0 ratio among systems and energies
- Constant value above $p_T = 3.5$ GeV/c
- Ratio reproduced by NLO calculations while not single spectra
- Observation of m_T scaling violation
  - Significance of 6.2σ below 3.5 GeV/c for pp at $\sqrt{s}$ = 8 TeV
- Hint of deviation from pp behavior at intermediate p_T in 0-10 % central in Pb-Pb at $\sqrt{s_{NN}}$ = 2.76 TeV

$\Rightarrow$ Importance of precise measurements

η/π^0 ratio in p-Pb at $\sqrt{s_{NN}}$ = 5.02 TeV

EPJ C78 (2018) no.8, 624

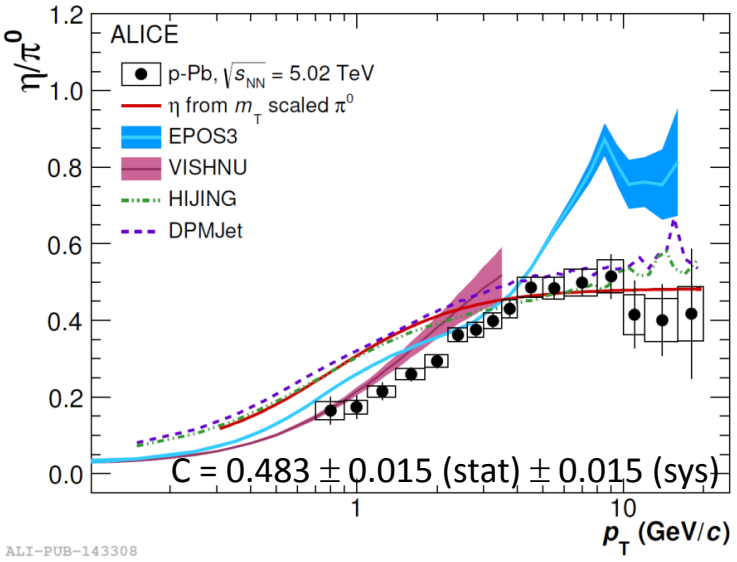

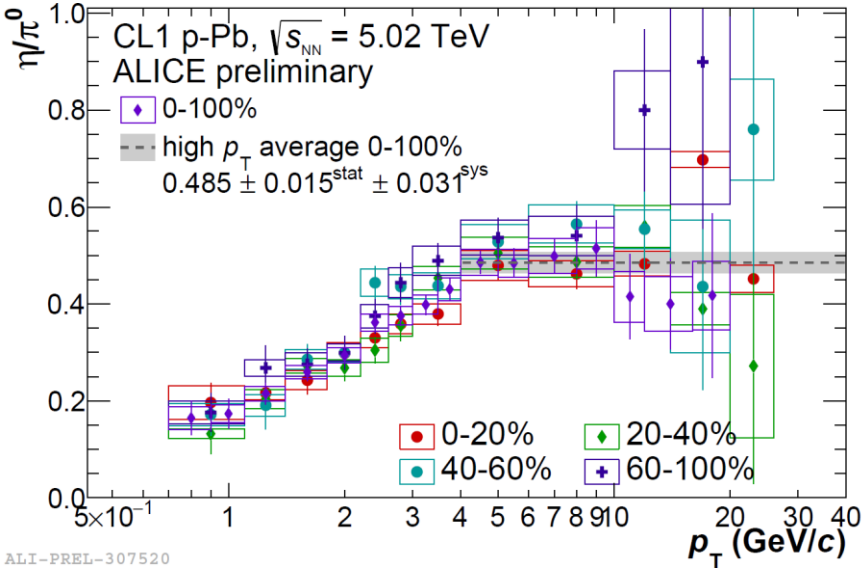

- m_T scaling violation at low p_T
- Same trend for HIJING, DPMJet and m_T scaling
- Good description by hydrodynamic models VISHNU and EPOS3 at low p_T
- Although, high p_T overshoot by EPOS3 (reflection of η spectrum prediction)
- No centrality dependence
- Difference between η/π^0 and $K^{\pm}/\pi^{\pm}$ ratio at low p_T

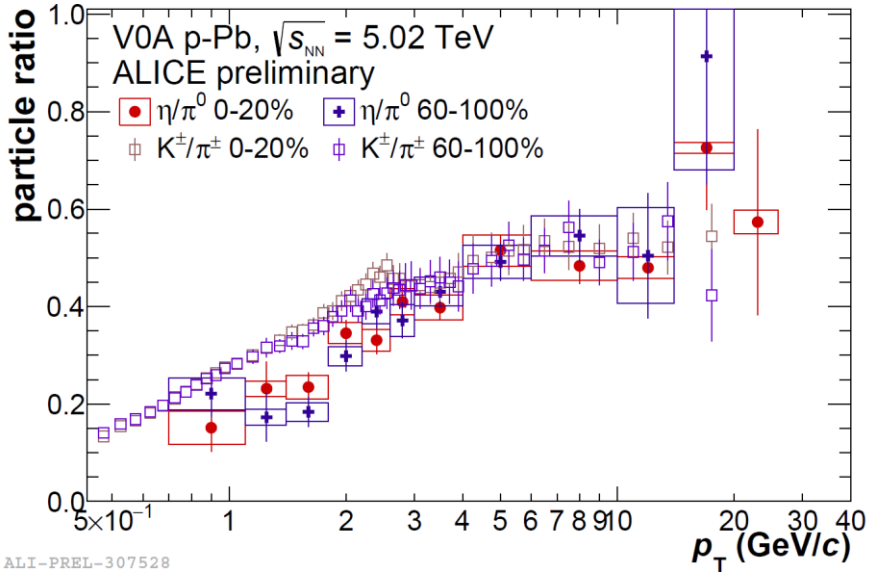

Nuclear modification factor

$$R_{AA}(p_T) = \frac{d^2N/dp_T dy|_{AA}}{\langle T_{AA}\rangle \times d^2\sigma/dp_T dy|_{pp}}$$

$N_{coll} = \sigma_{pp} \langle T_{AA} \rangle$

- Illustrates medium effect
- Contains both initial and final state effect
  - Initial state: i.e. Cronin, nuclear shadowing
  - Final state: collisional and radiative energy loss
- $R_{AA} = 1 \rightarrow$ no modification

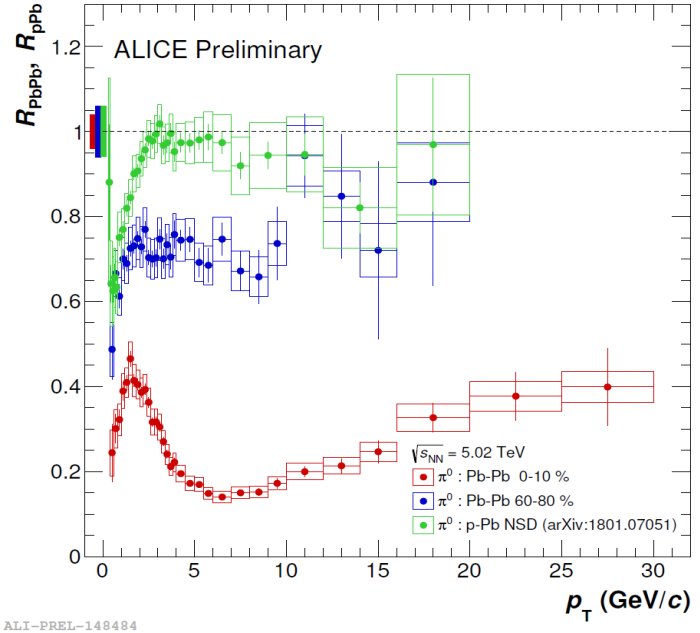

- Well defined fragmentation function in comparison to unidentified hadrons
- Very strong suppression (R_{AA} ~ 0.1) in central Pb-Pb collisions above $p_T \approx 3$ GeV/c

  $\Rightarrow$ Formation of hot and dense QCD matter
- Centrality dependence
- Similar suppression for two Pb-Pb collision energies
- Consistent with unity above 2 GeV/c for p-Pb
- Agreement with results for charged hadrons

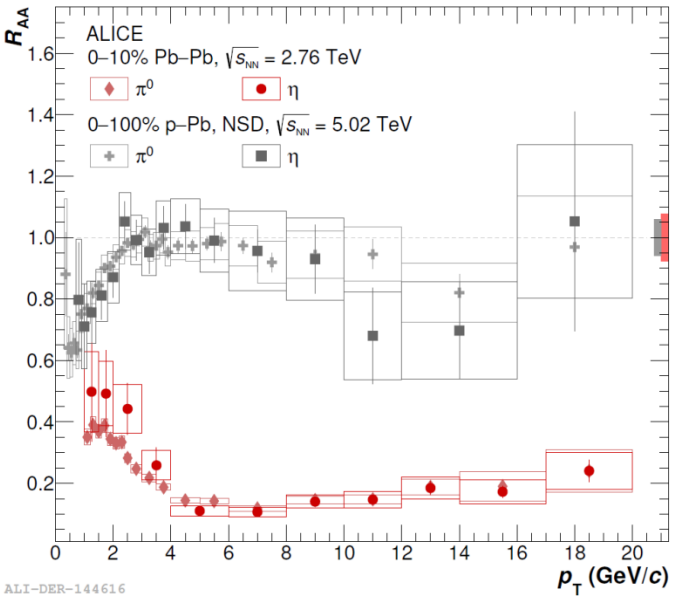

$\sqrt{s_{NN}}$ dependence of the π^0 R_{AA}

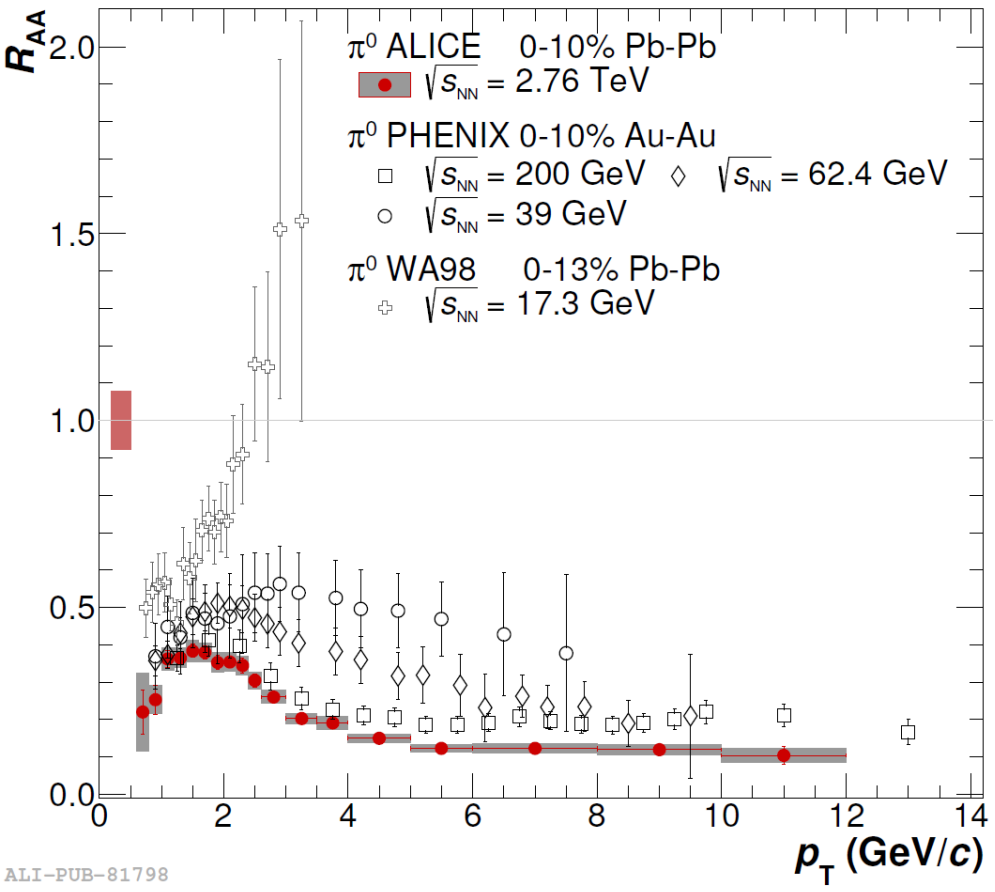

- Similar shape of π^0 R_{AA} for $\sqrt{s_{NN}}$ = 2.76 TeV and $\sqrt{s_{NN}}$ = 200 GeV
- The higher center of mass energy the larger suppression
- Onset of suppression between $\sqrt{s_{NN}}$ = 17.3 GeV and $\sqrt{s_{NN}}$ = 39 GeV

ALICE: EPJC 74 (2014) 10, 3108
PHENIX: PRL 109 (2012) 152301
PHENIX: PRL 101 (2008) 232301
WA98: PRL 100 (2008) 242301

Neutral meson R_{AA} in Pb-Pb at $\sqrt{s_{NN}}$=2.76 TeV

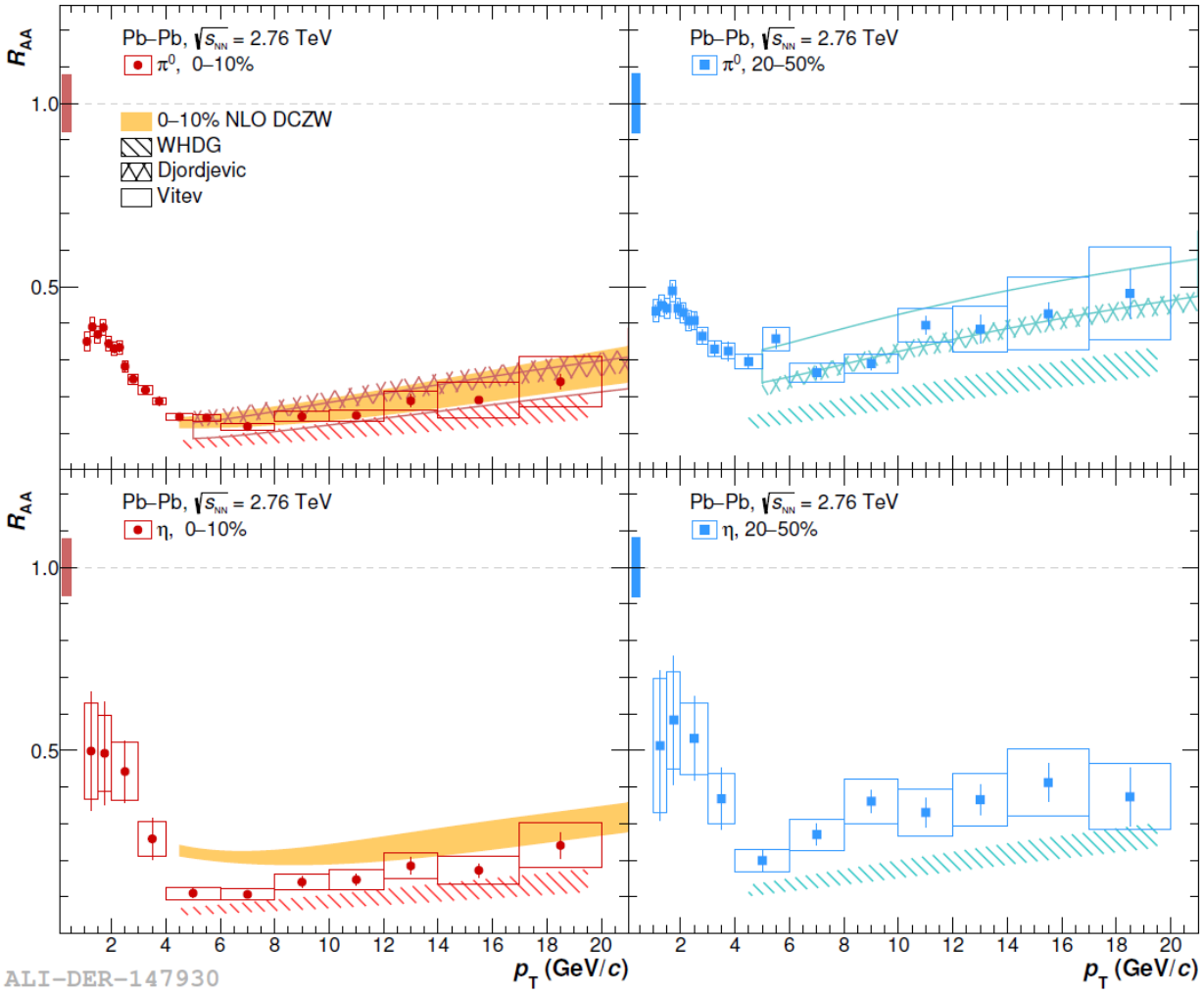

NLO DCZW :
Phys. Lett. B750 (2015) 390-395
WHDG :
Int. J. Mod. Phys. E16 (2007) 2193-2199
Djordjevic :
Phys. Lett. B734 (2014) 286-289
Vitev et al.:
Phys. Rev. D 93, 074030 (2016)

- NLO DCZ describes suppression in central Pb-Pb collsions for π^0 but overpredicts η
- Vitev and Djordjevic describe both centralities for π^0
- WHDG model predictions lie below measurements

π^0 meson R_{AA} in Pb-Pb at $\sqrt{s_{NN}}$ = 5.02 TeV

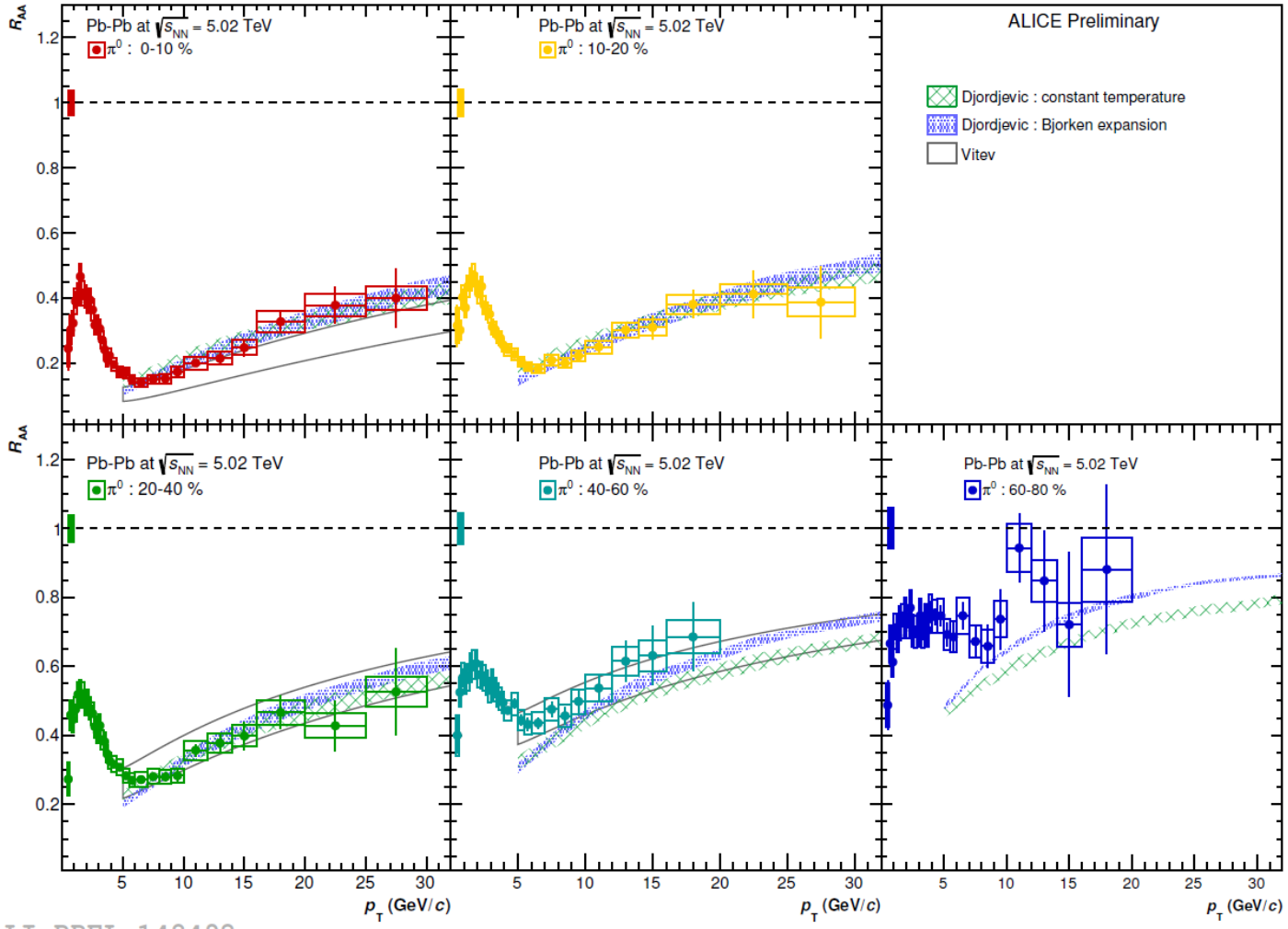

Djordjevic:
PRC94 (2016) 044908
Energy loss in evolving finite-size QGP

Vitev:
PRD93 (2016) 074030
Soft-Collinear effective theory for jet propagation in matter

- Relatively well description by models
- Centrality dependence reproduced
- Although worsening towards more peripheral collisions

Q_{pA} centrality dependence

$$Q_{pA}(p_T) = \frac{\frac{1}{N_{evt}^{pA}} d^2N^{pA}(p_T)/d\eta dp_T}{\langle N_{coll}\rangle \frac{1}{N_{evt}^{pp}(p_T)} d^2N^{pp}/d\eta dp_T}$$

ZNA: |η|>8.7, Pb side
V0A: 2<|η|<5.1, Pb side
CL1: |η|<1.4

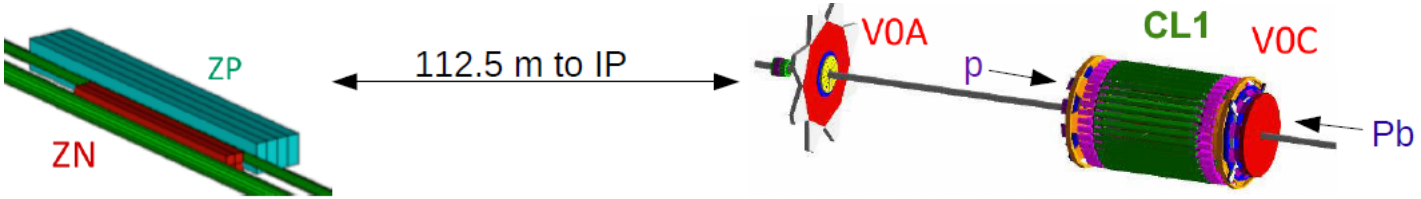

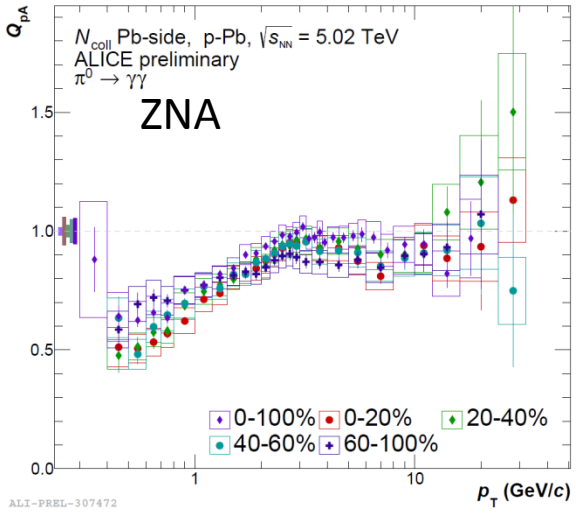

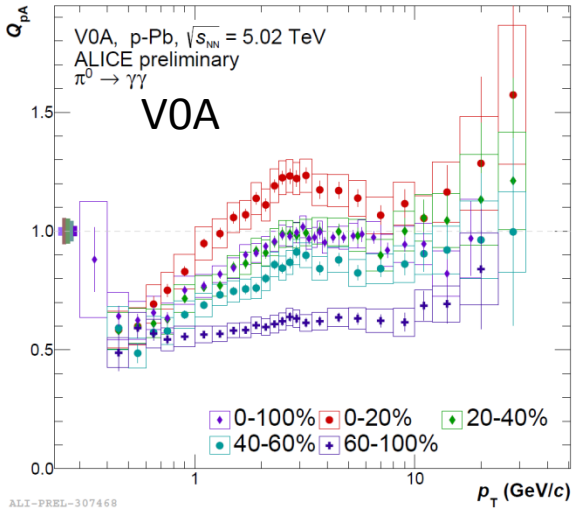

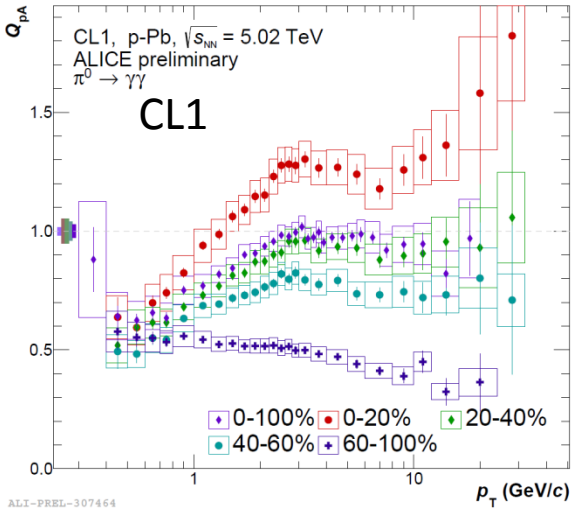

- No strong centrality dependence for ZNA estimator
- Strong and similar dependence for V0A and CL1 estimators

Particle dependence of Q_{pA}

h±: PRC91 (2015) 064905
D0: JHEP 1608 (2016) 078

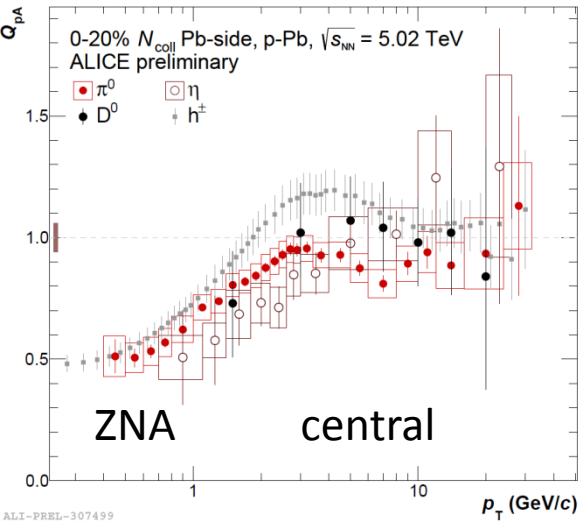

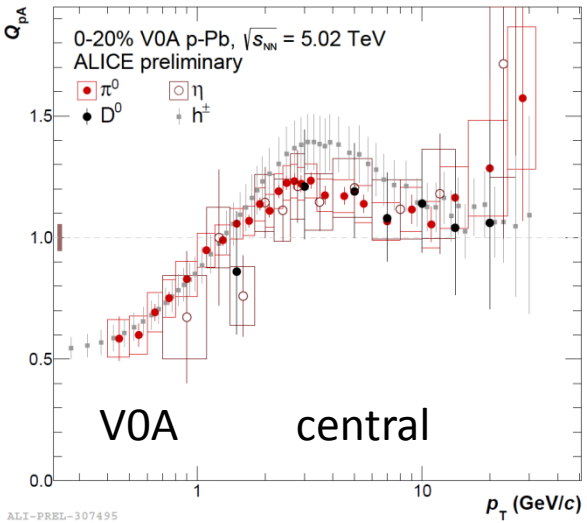

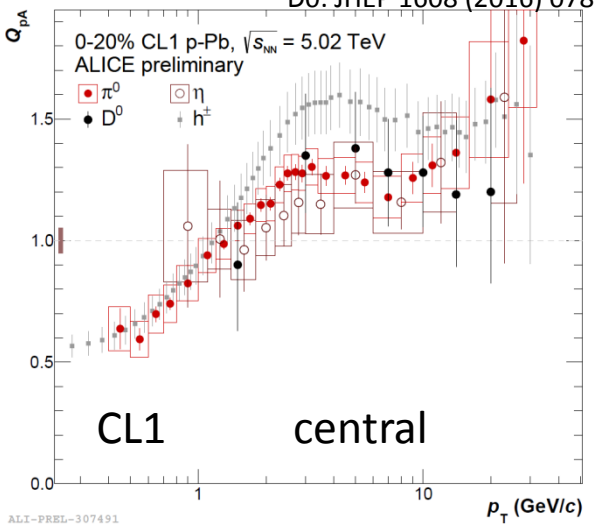

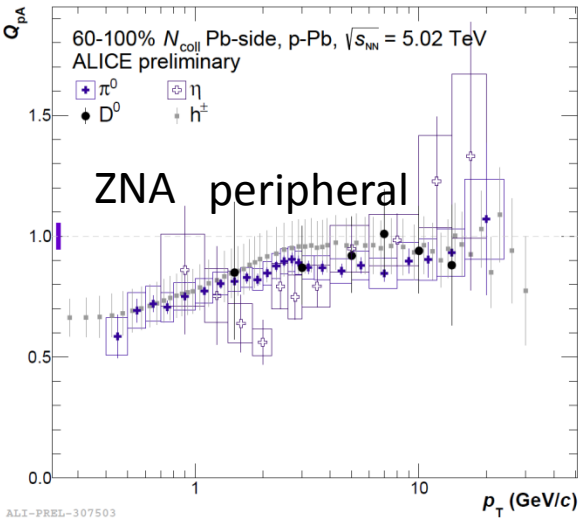

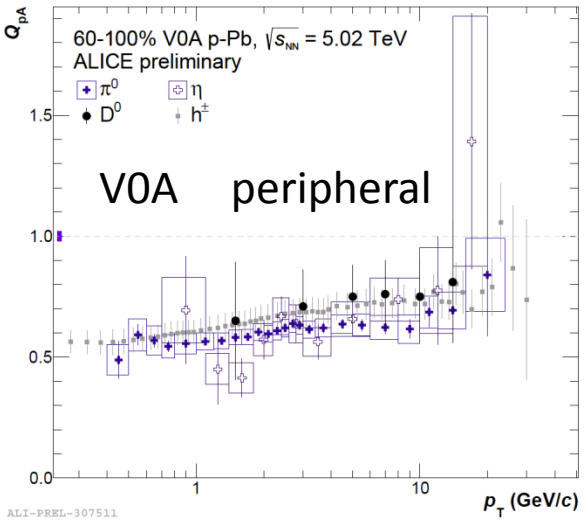

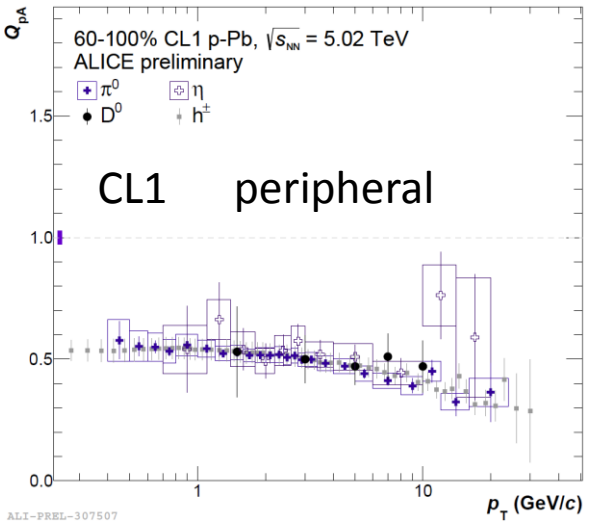

- Similar trend for π^0 and η mesons for every estimator and centrality class
- Bump around $p_T \approx 3$ GeV/c for $h^{\pm}$ (protons?)
- D^0 mesons consistent with neutral mesons

Particle dependence of R_{AA}

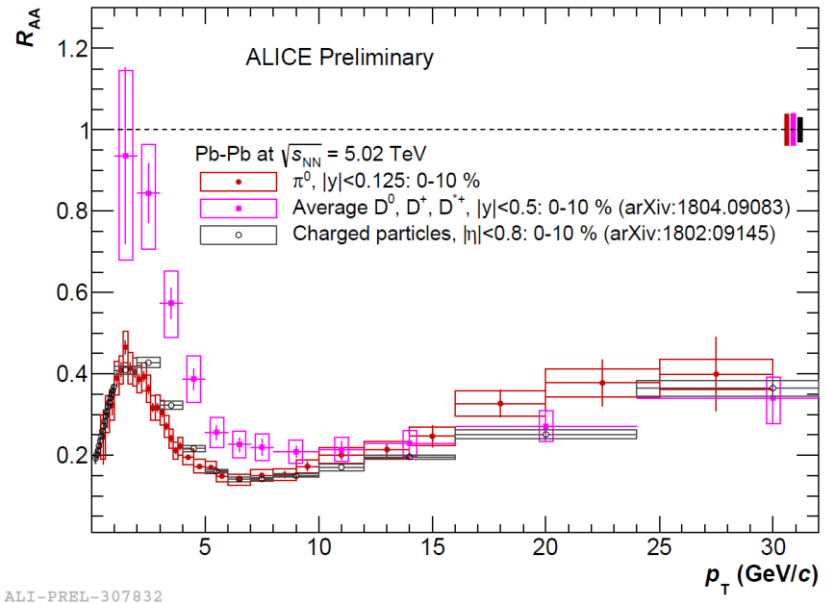

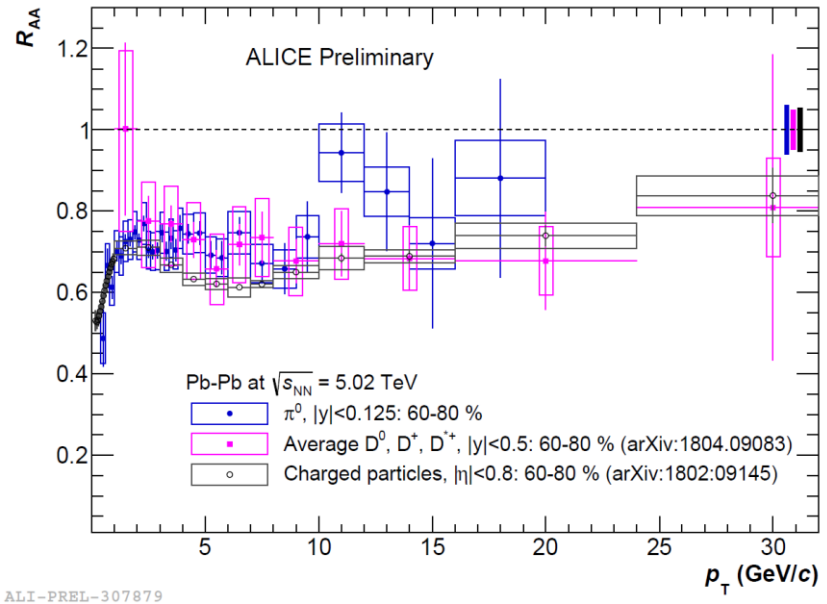

- Similar suppression above $p_T \approx 10$ GeV/c
- Similar suppression for neutral pions and charged hadrons
- Hierarchy in suppression (R_{AA}(D)>R_{AA}(π)) at low p_T?
  - Recombination
  - Quark masses
  - Different flow
  - Other

Summary

- ALICE can measure neutral mesons in wide p_T range
- Measurements allow testing perturbative QCD inspired models and parameterization of parton distribution and fragmentation functions
  - Higher yield predicted by NLO pQCD for π^0 (by 20-60%) and η (by 50-100%)
- Significant m_T scaling violation was observed at p_T<3 GeV/c for pp, p-Pb and Pb-Pb collisions
- π^0 and η meson spectra measured in p-Pb at $\sqrt{s_{NN}}$=5.02 TeV
  - In four centrality classes
  - Three centrality estimators
  - Strong dependence of Q_{pA} on rapidity gap to centrality estimator
- π^0 yield measured in Pb-Pb at $\sqrt{s_{NN}}$=2.76 and 5.02 TeV
  - Several centrality classes
  - R_{AA} for two energies are very close between each other
  - Models of Vitev and Djordjevic reproduce centrality and p_T dependence
- π^0 and η Q_{pA} consistent with D mesons but R_{AA} (π) smaller than R_{AA}(D)

Backup

π^0 production spectrum in pp @ 5 TeV comparison

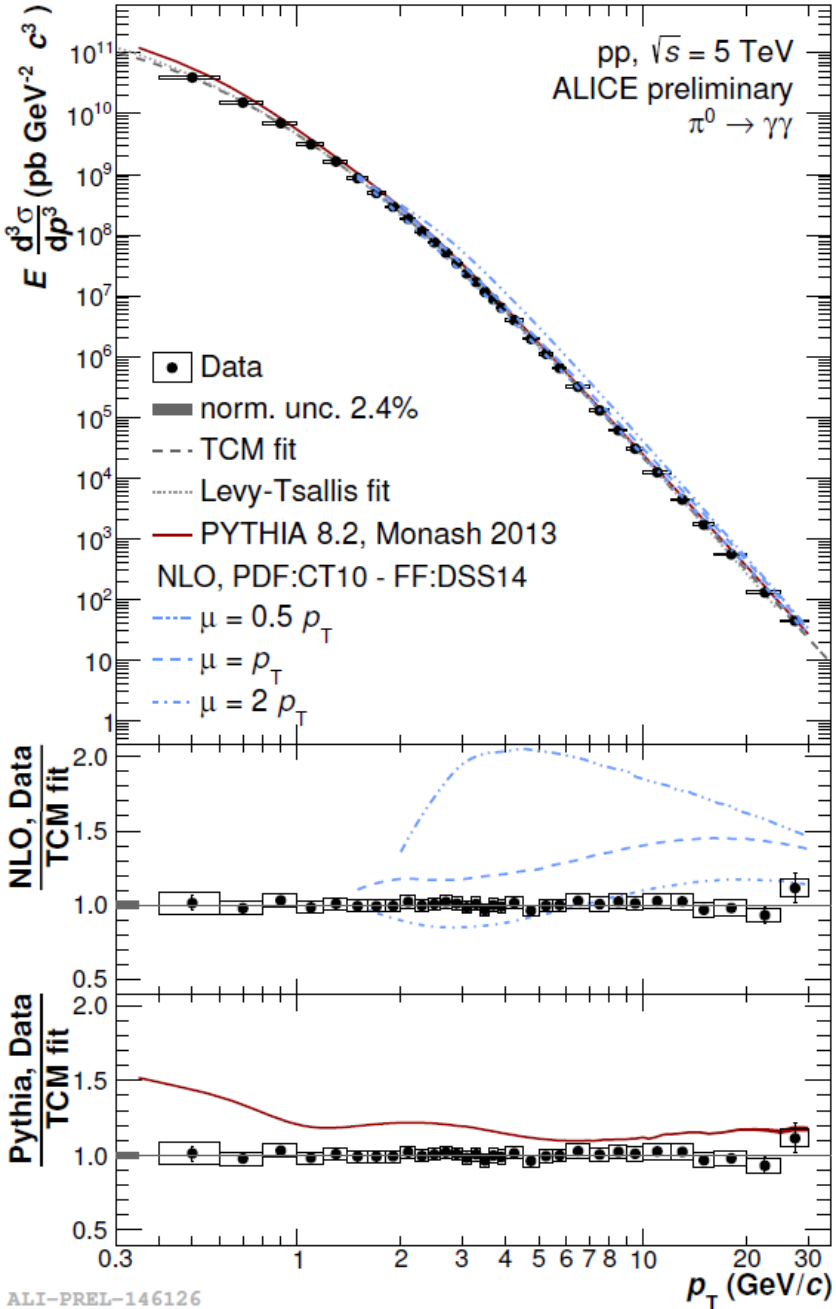

ALICE detector - 2012

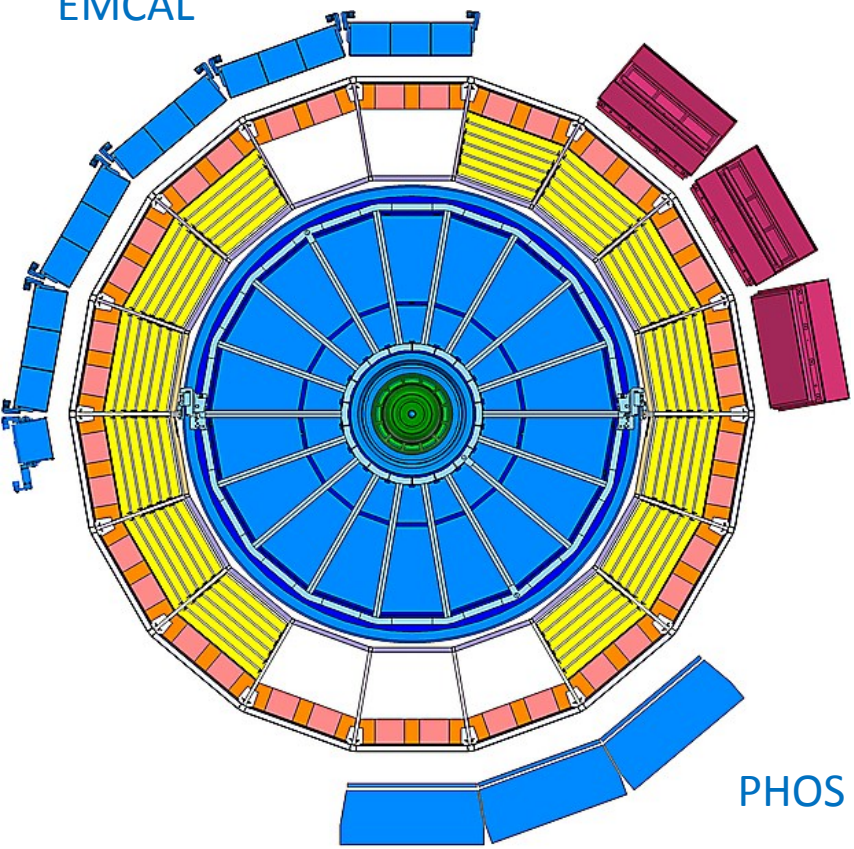

EMCAL:

- 12 SM* (10 + 2 × 1/3)
- $|\eta| < 0.7$
- $80° < \varphi < 187°$ $(\Delta\varphi = 107°)$

PHOS:

- 3 SM
- $|\eta| < 0.12$
- $260° < \varphi < 320°$ $(\Delta\varphi = 60°)$

*10 SM are in readout

- Run I – 2012
- pp @ 8 TeV, p-Pb @ 5.02

R_{AA} for p-Pb and Pb-Pb

PRL 110, 082302 (2013)

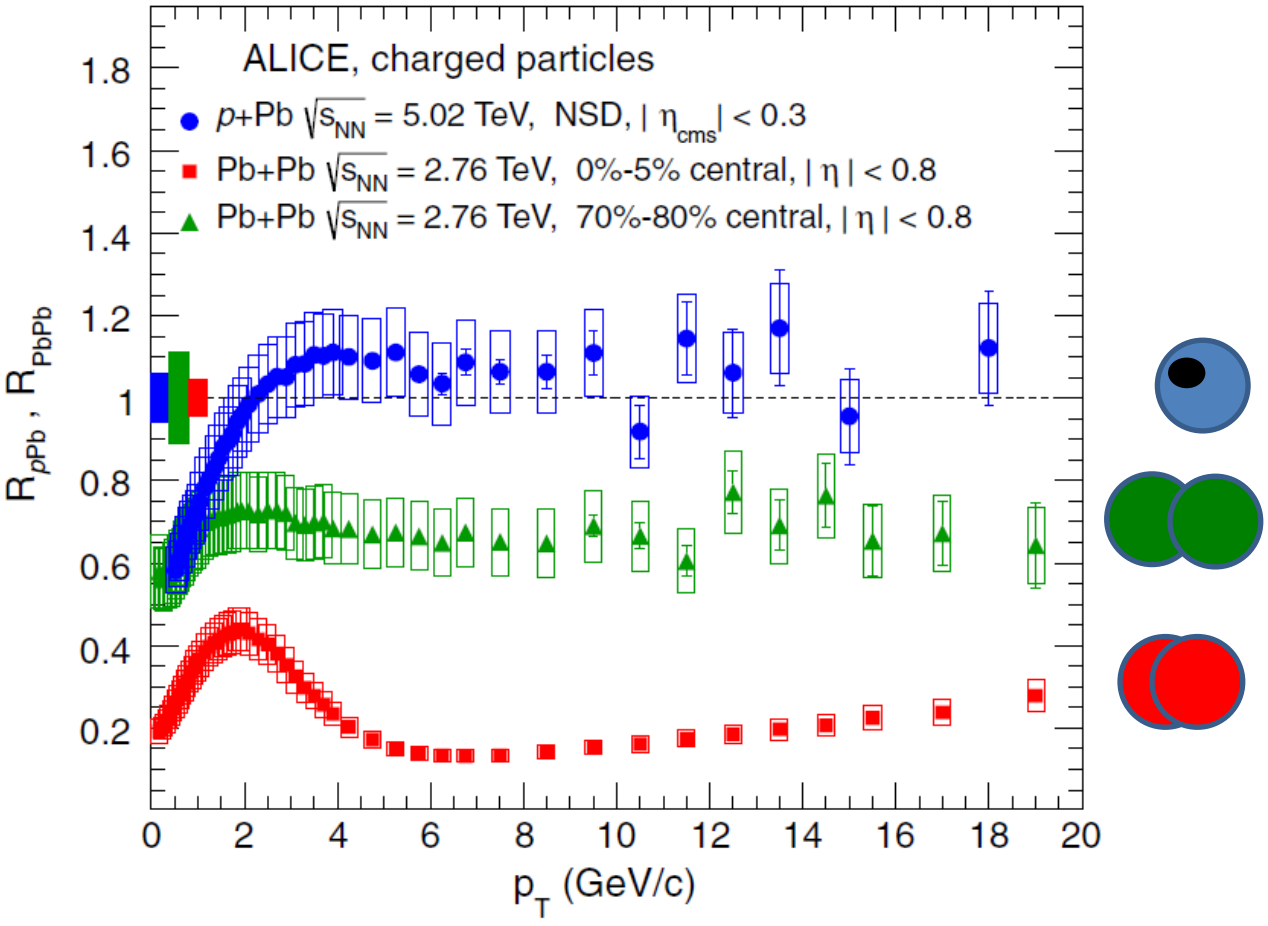

Centrality estimation in Pb-Pb

- Centrality observables
  - Charge particle multiplicity in VZERO
  - Forward energy in ZDC
  - SPD for systematics
- Number of particle sources

  $f \times N_{part} + (1 - f) \times N_{coll}$
- Number of particles produced by each source given by Negative Binomial Distribution (μ, κ)
- Glauber model fits to cross-section
  - 100% trigger efficiency
  - Background is negligible

  $\rightarrow$ ~ 90% of total cross-section

  with $\sigma_{INEL}^{NN} = 64 \pm 5$ mb

  <1% agreement (0-70%) N_{part} with Glauber fit

  3.5 % for peripheral (>70%)
- Define centrality classes corresponding to fractions of the inelastic Pb-Pb cross-section

Phys. Rev. C 88, 044909 (2013)

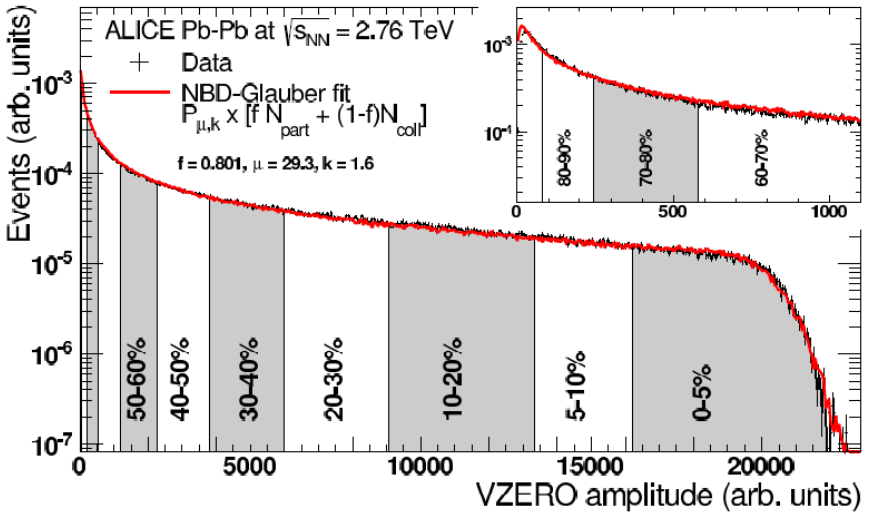

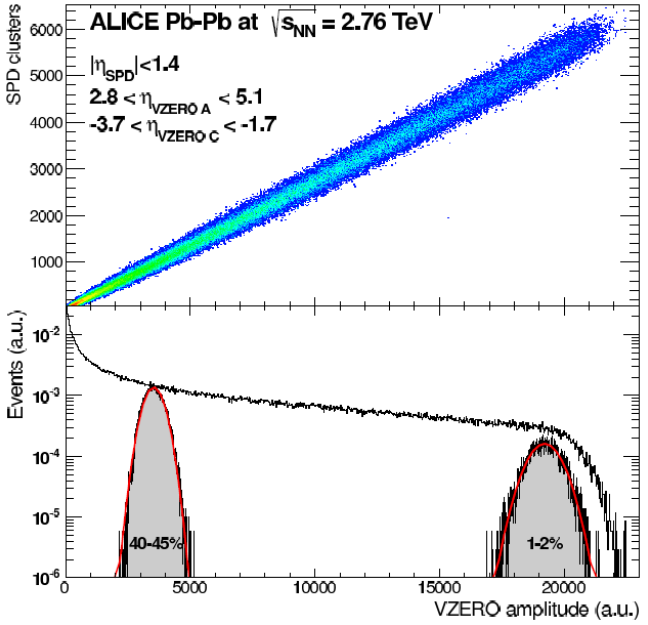

Functions

- Tsallis

$$f(p_T) = \frac{1}{2\pi}\frac{dN}{dy}\frac{(n-1)(n-2)}{nT(nT+m(n-2))}\left(1+\frac{\sqrt{p_T^2+m^2}-m}{nT}\right)^{-n}$$

$$E\frac{d^3\sigma^{pp\to\pi^0X}}{dp^3} = \frac{\sigma_{pp}^{INEL}}{2\pi}A\frac{(n-1)(n-2)}{nC[nC+m(n-2)]}\left(1+\frac{m_T-m}{nC}\right)^{-n}$$

- Hagedorn

$$E\frac{d^3\sigma^{pp\to\pi^0X}}{dp^3} = \left(\frac{p_0}{p_0-p_T}\right)^n$$

- Power law

$$E\frac{d^3\sigma^{pp\to\pi^0X}}{dp^3} = c\left(\frac{1}{p_T}\right)^n$$

- Two Component Model (TCM)

$$\frac{1}{2\pi N_{\mathrm{ev}}}\frac{\mathrm{d}^2N}{p_{\mathrm{T}}\mathrm{d}p_{\mathrm{T}}\mathrm{d}y} = A_{\mathrm{e}}\exp\left(-E_{\mathrm{T,kin}}/T_{\mathrm{e}}\right) + A\left(1+\frac{p_{\mathrm{T}}^2}{T^2n}\right)^{-n}$$

Meson production in pp at $\sqrt{s}$ = 8 TeV

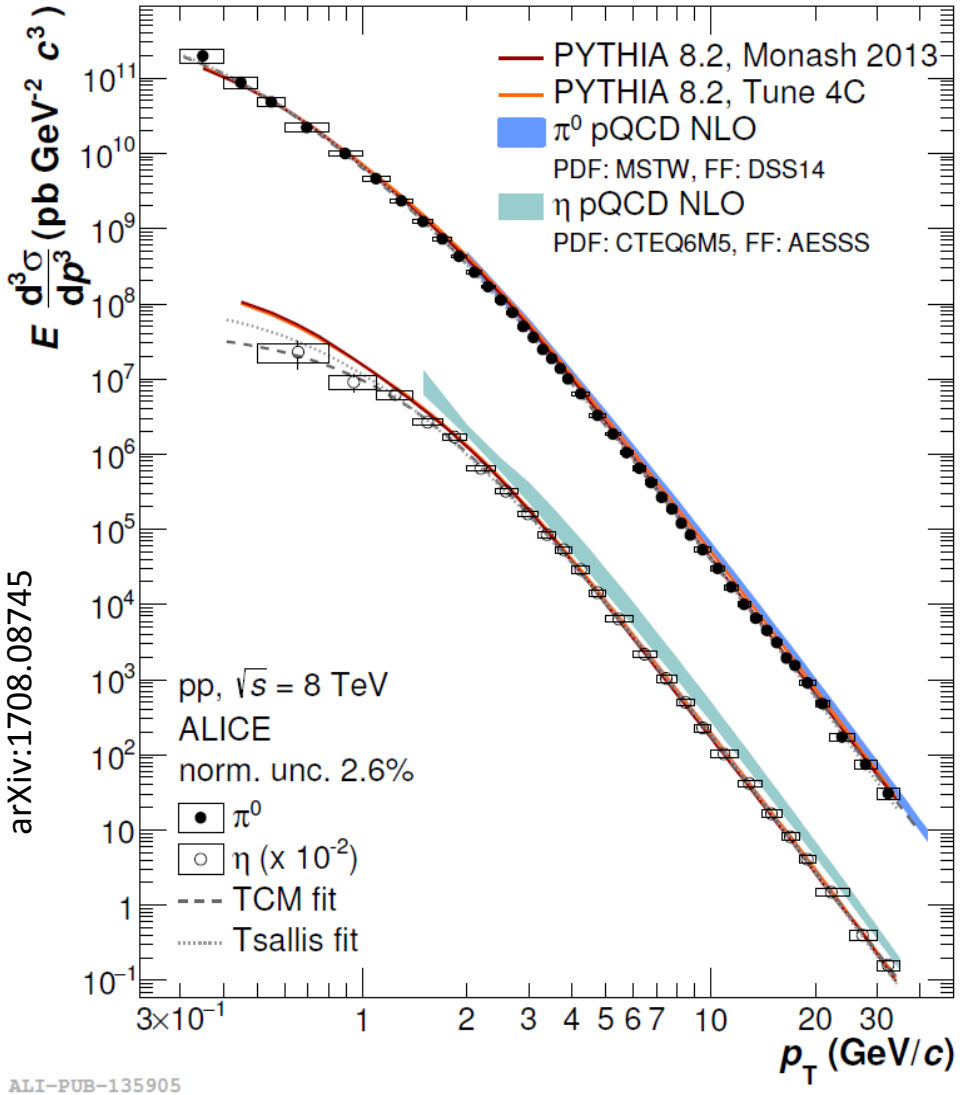

arXiv:1708.08745

- Wide p_T range:
  - $0.3 < p_T < 35$ GeV/c (π^0)
  - $0.5 < p_T < 35$ GeV/c (η)
- Data described by many functions: Tsallis, TCM
- NLO pQCD calculations overshoot data

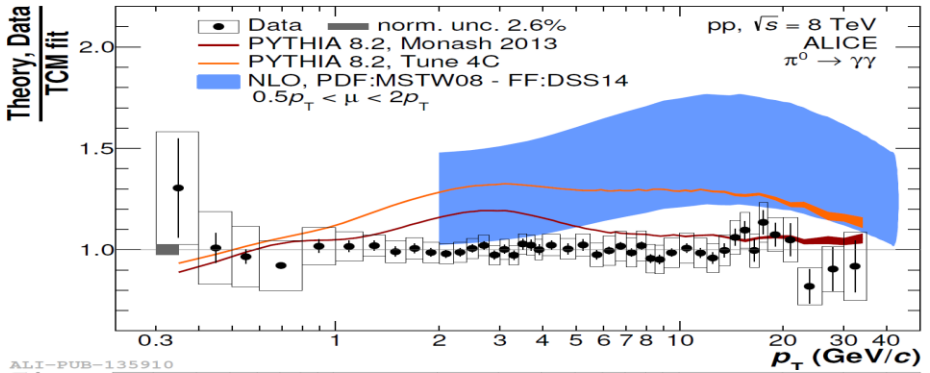

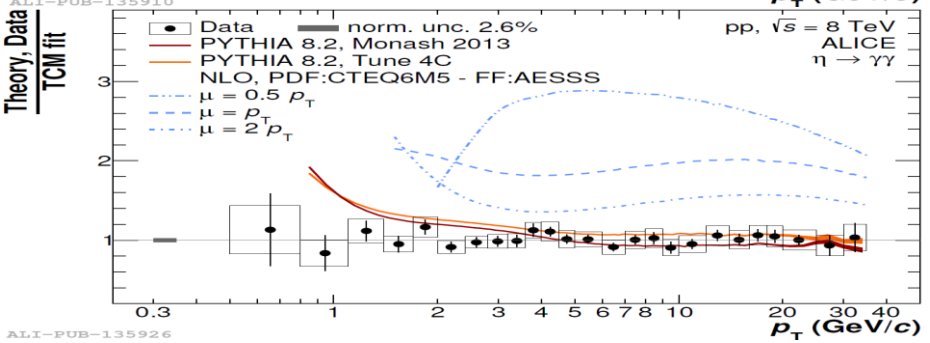

Meson production in pp at $\sqrt{s}$ = 2.76 TeV

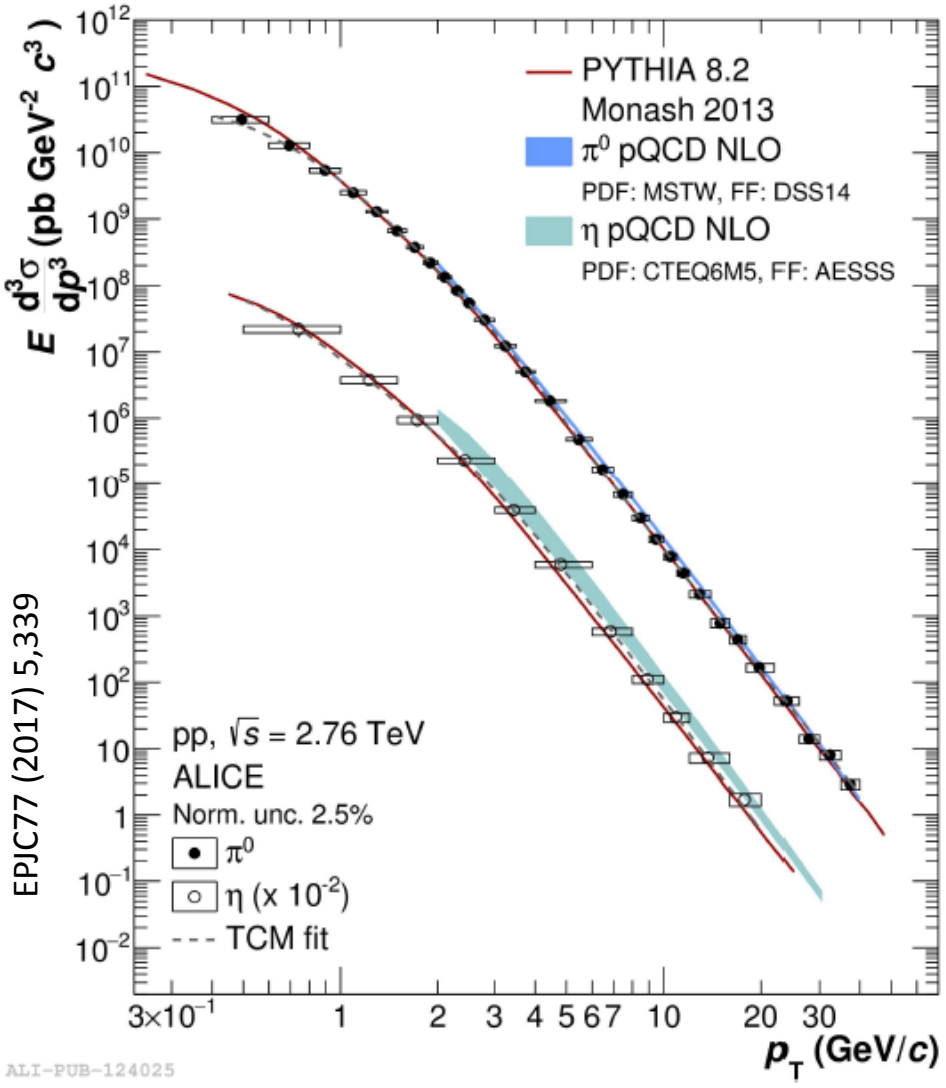

- Extended wide p_T range:
  - $0.4 < p_T < 40$ GeV/c (π^0)
  - $0.5 < p_T < 20$ GeV/c (η)
- Improved reference for Pb-Pb data
- Data described by many functions: Tsallis, TCM
- NLO pQCD calculations overshoot data

π^0 spectra in Pb-Pb @ $\sqrt{s_{NN}}$ = 2.76 TeV, new result

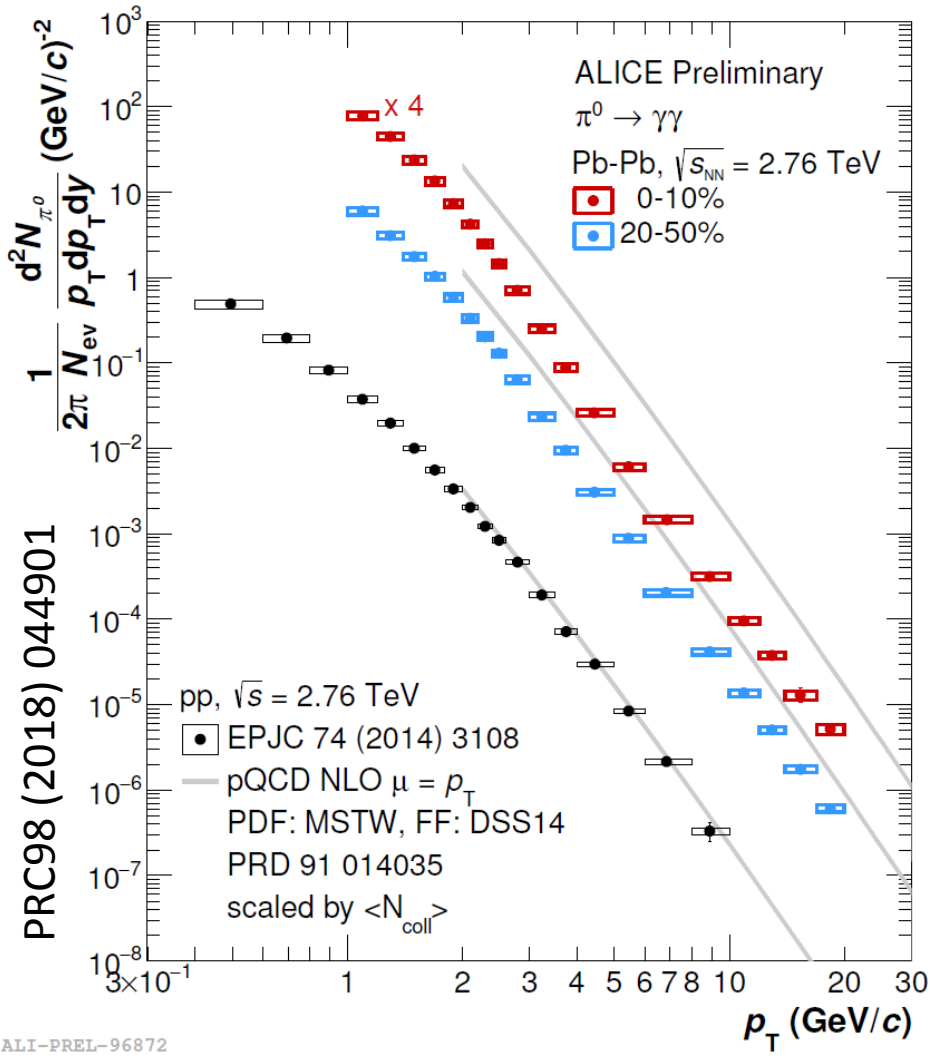

- 10 times more statistics in 2011 (L ~ 0.1 nb^{-1})
- Extended p_T range up to 20 GeV/c
- Two complementary analyses methods: EMCal and PCM
- Two centrality classes compared to pp
- Compared to NLO pQCD pp predictions scaled by N_{coll} (PRD 91 (2015) 1, 014035)

η spectra in Pb-Pb @ $\sqrt{s_{NN}}$ = 2.76 TeV

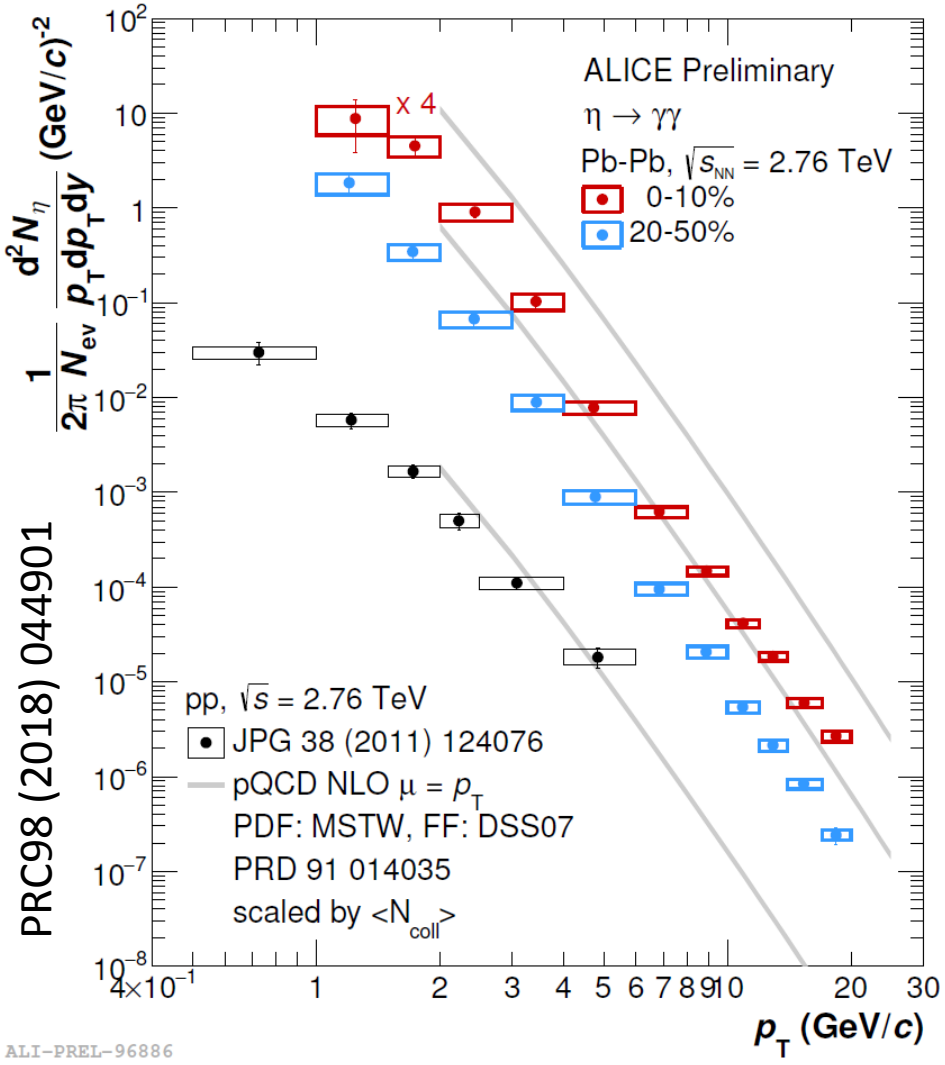

- First η measurement in Pb-Pb at the LHC
- Range: $1 < p_T < 20$ GeV/c
- Two complementary systems: EMCal and PCM
- Two centrality classes compared to pp
- Compared to η production of NLO pQCD pp predictions scaled by N_{coll} (PRD 91 (2015) 1, 014035)

π^0 spectra in Pb-Pb @ 5.02 TeV

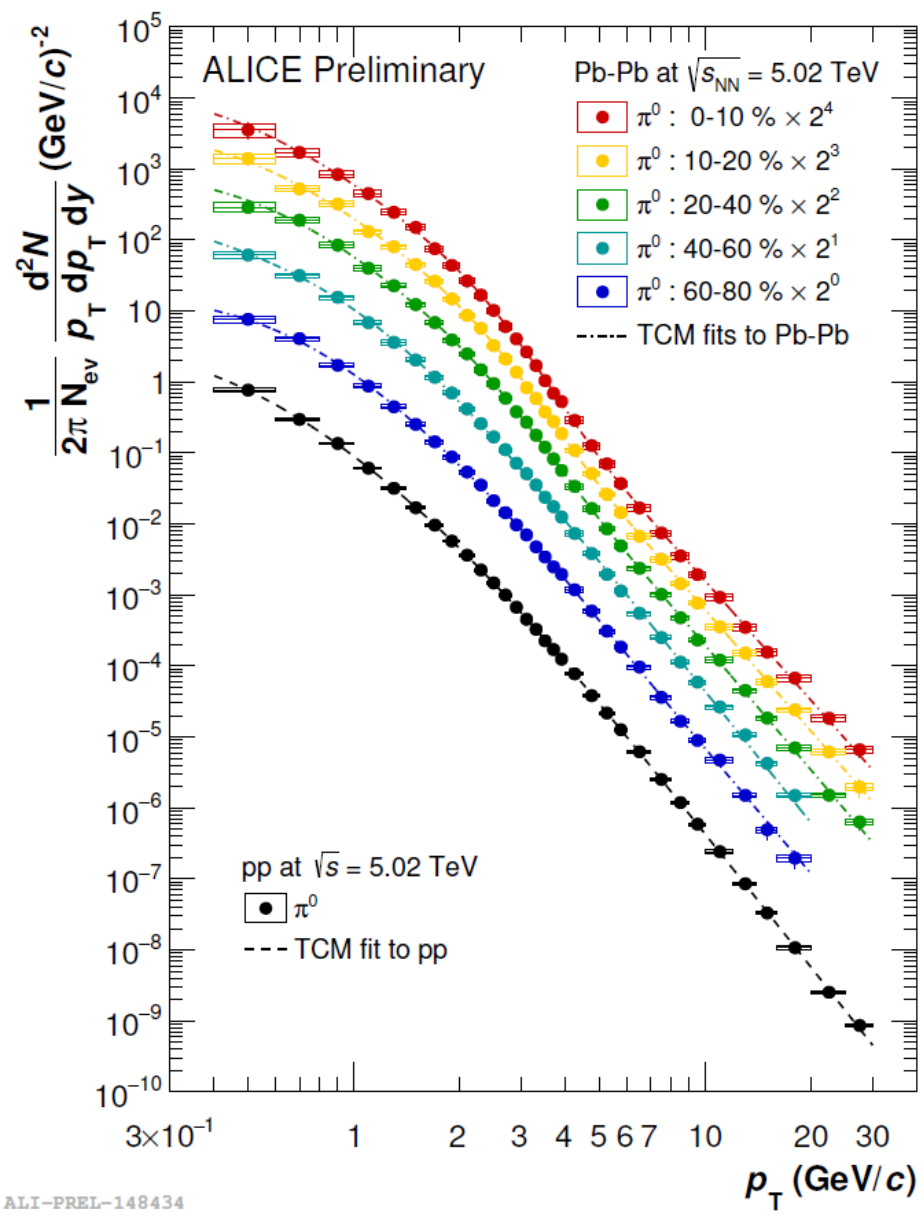

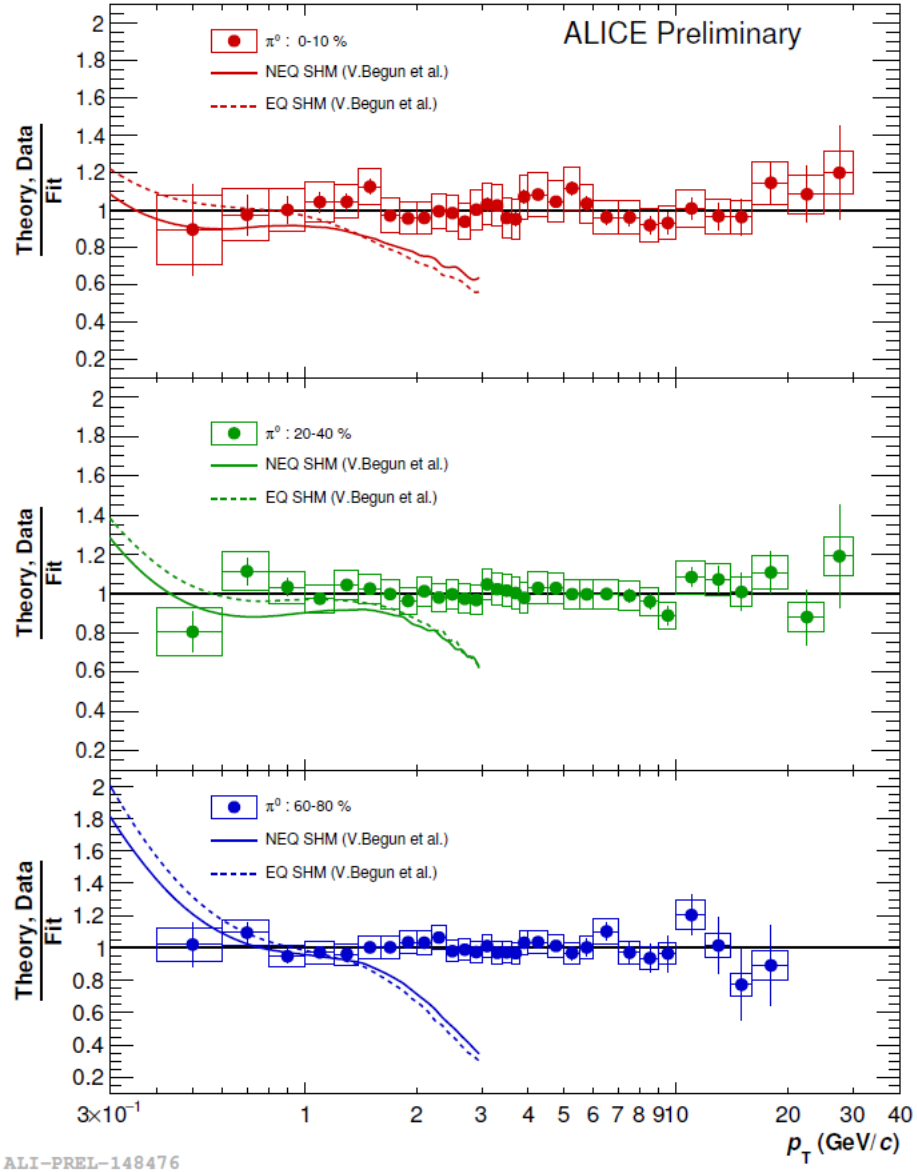

$$M_{\gamma\gamma} = \sqrt{2E_1E_2(1-\cos\theta_{12})}$$

Invariant mass

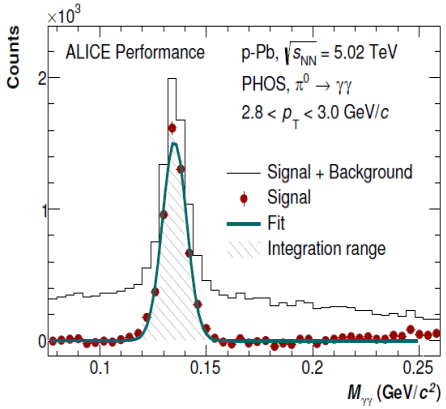

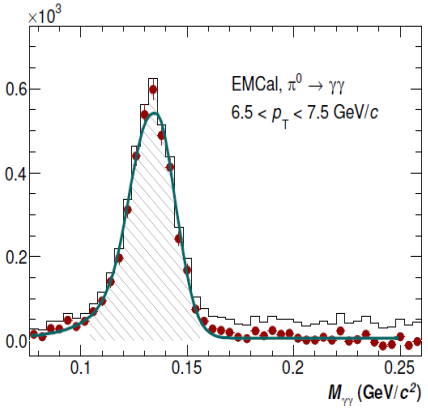

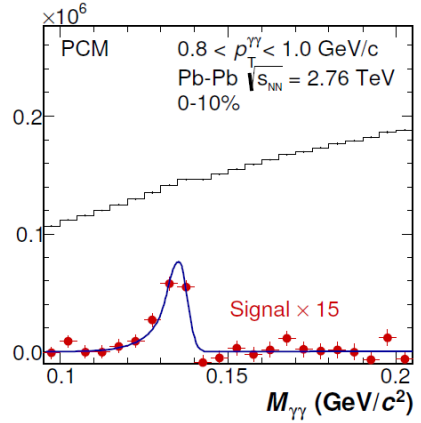

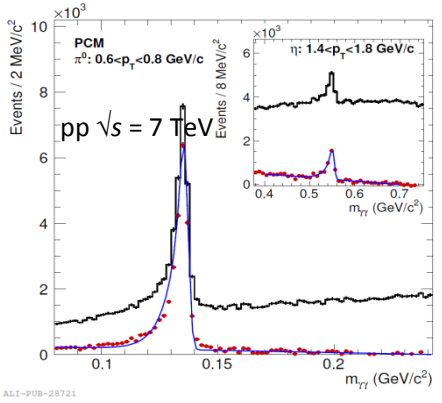

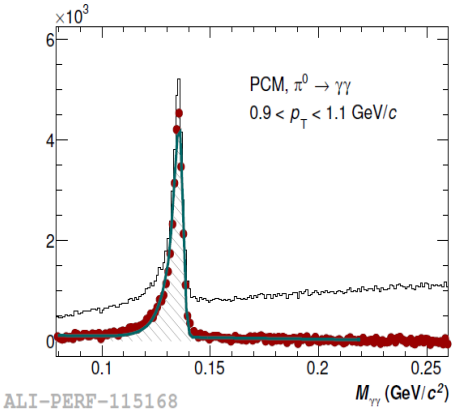

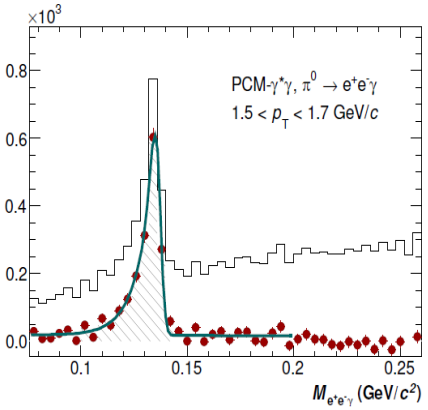

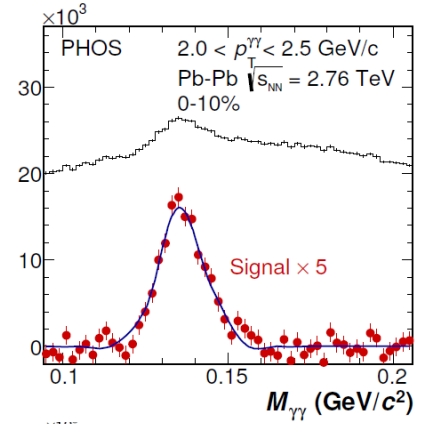

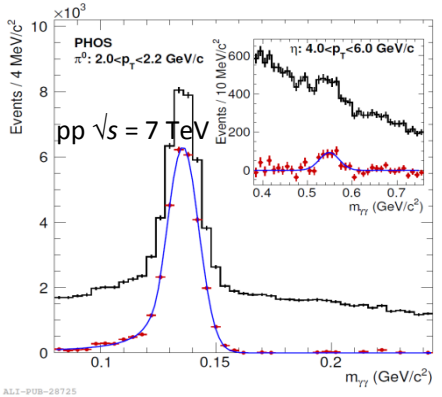

EPJ C (2014) 74:3108 PLB 717 (2012) 162-172

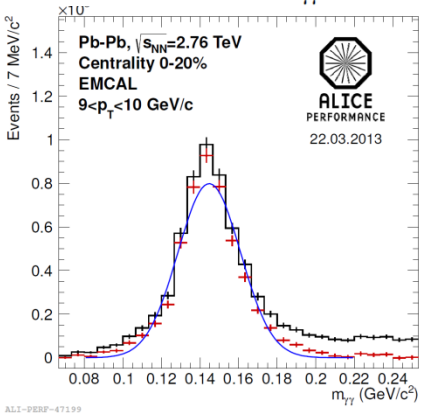

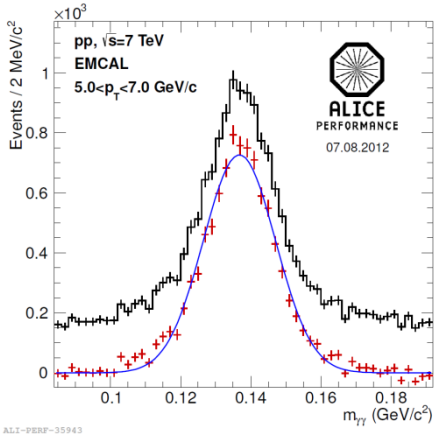

π^0 is reconstructed

- For different collision energies
- In different systems (pp, p-Pb, Pb-Pb)
- Via different methods (detectors)
- In wide p_T range

Good agreement between methods allowed for combined result

Invariant mass

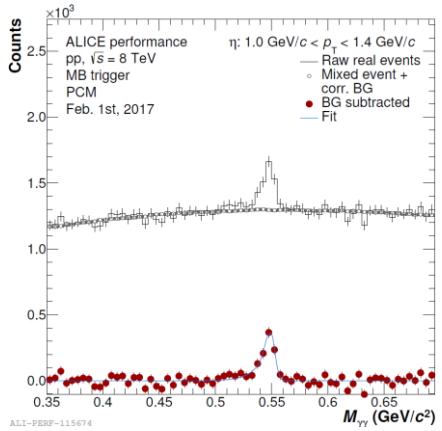

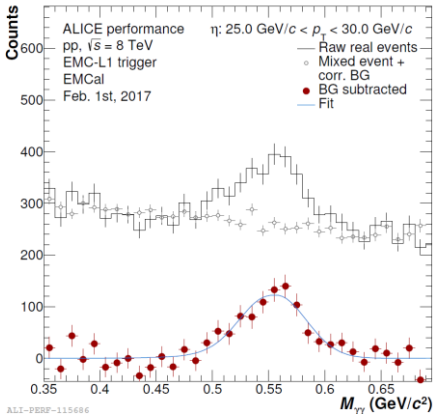

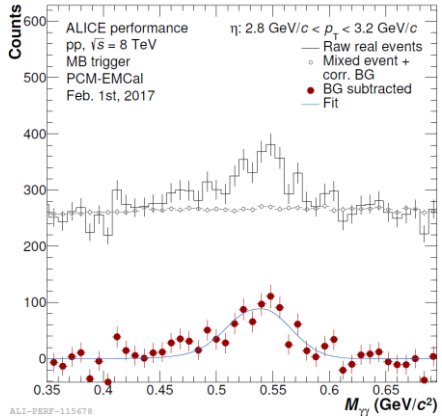

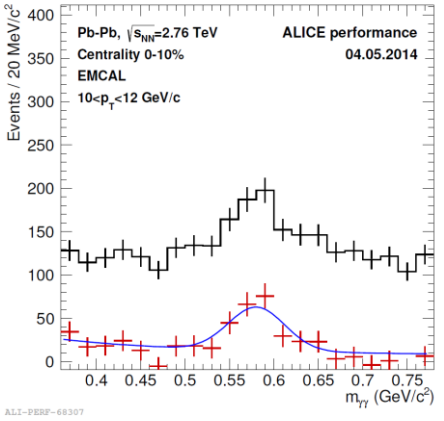

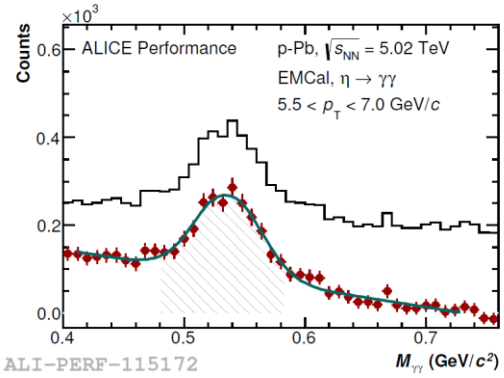

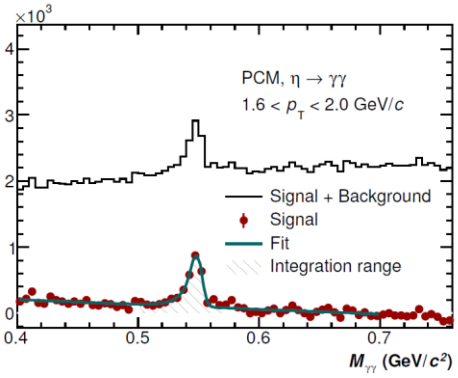

Meson reconstruction

- Invariant mass

$$M_{\gamma\gamma} = \sqrt{2E_1E_2(1-\cos\theta_{12})}$$

- Event mixing to reduce combinatorial background
- Signal (exponent + Gaussian) and background (polynomial) parameterization
- Bin counting for raw yields
- Corrections based on MC

$$E\frac{\mathrm{d}^3\sigma}{\mathrm{d}p^3} = \frac{N_{\mathrm{rec}}}{p_{\mathrm{T}}^{*}\,\Delta p_{\mathrm{T}}\,\varepsilon\,\varepsilon_{\mathrm{trig}}}\,\frac{1}{L_{\mathrm{int}}}\,\frac{1}{\mathrm{BR}}$$

Mesons R_{AA} in p-Pb @ 5.02 TeV

EPJC 78 (2018) 624

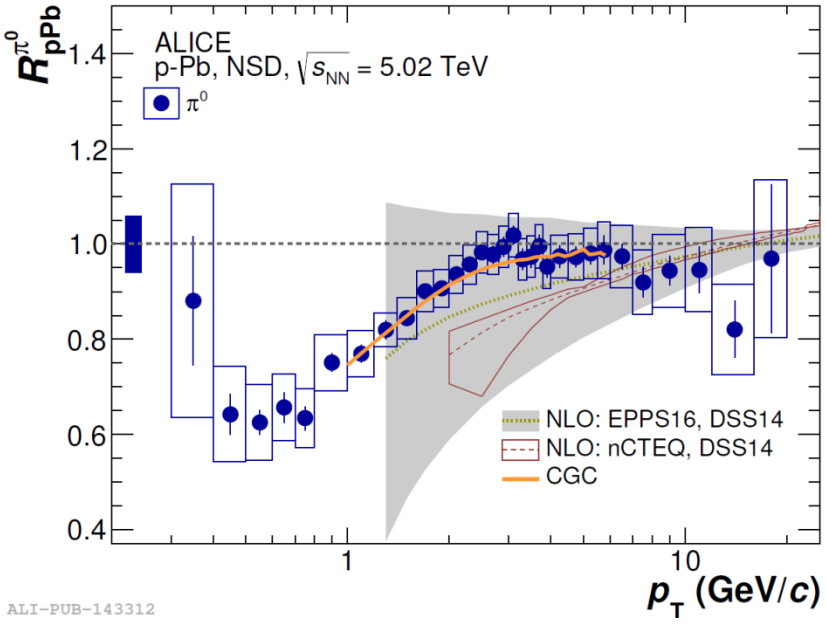

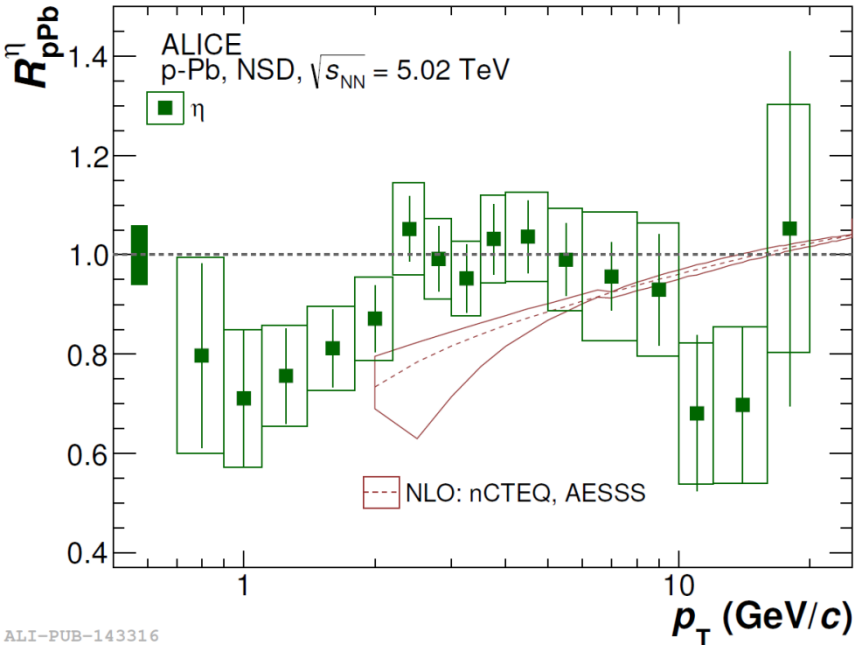

η/π^0 ratio

EPJC 77 (2017) 5,339

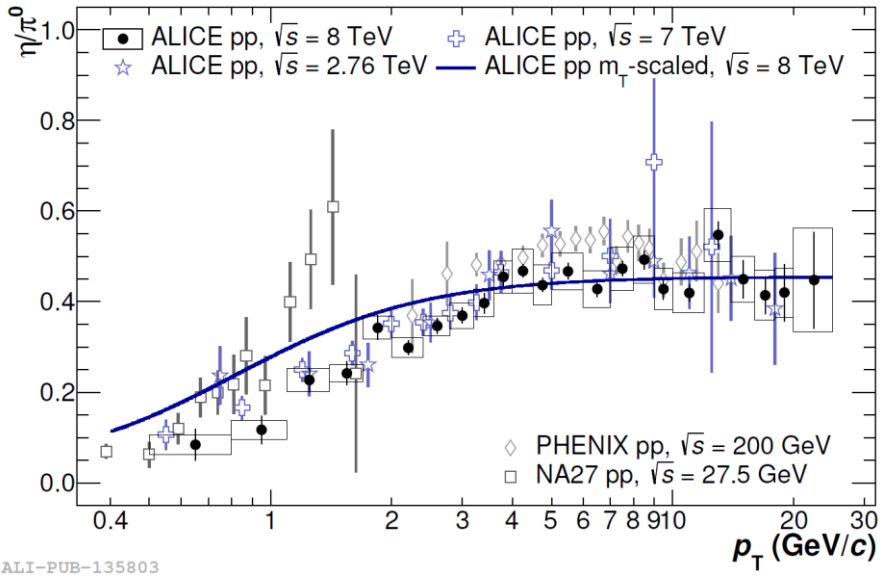

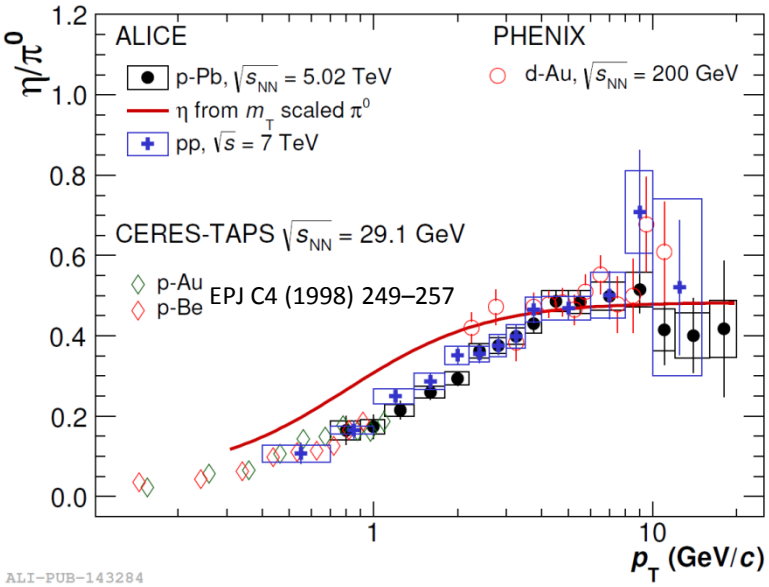

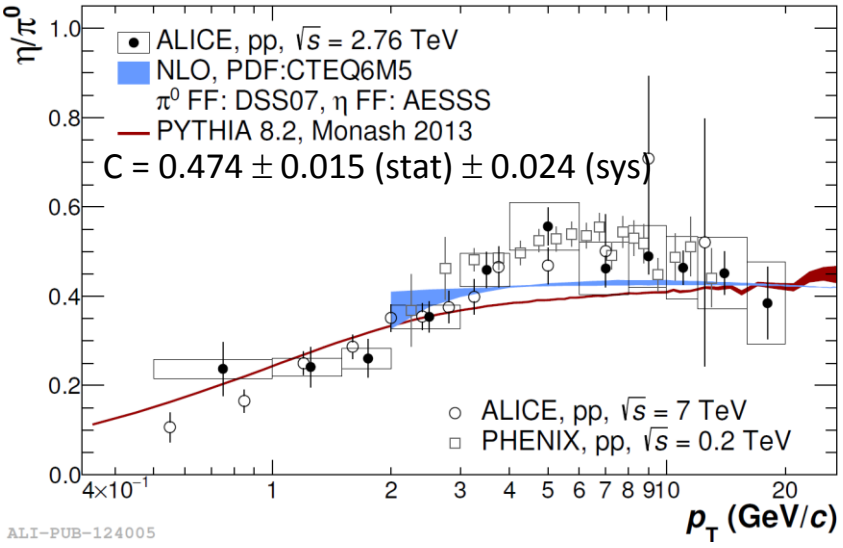

η/π^0 ratio in Pb-Pb @ $\sqrt{s_{NN}}$ = 2.76 TeV

PRC98 (2018) 044901

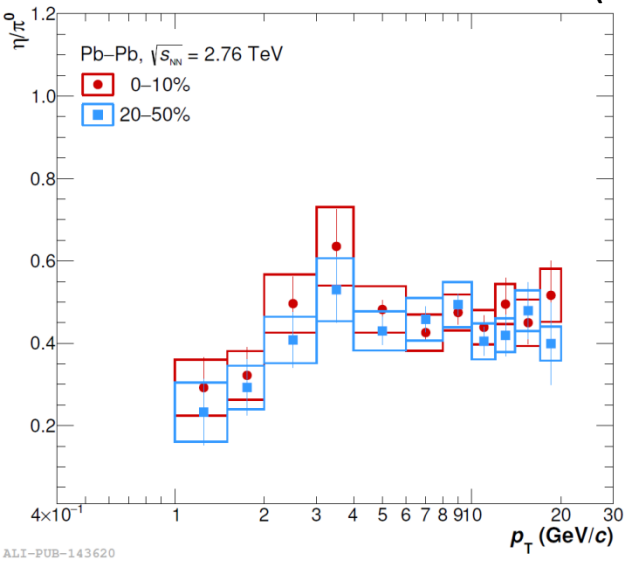

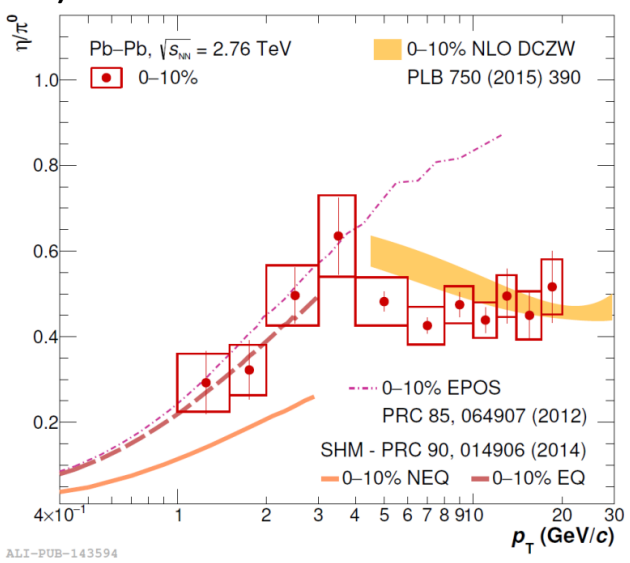

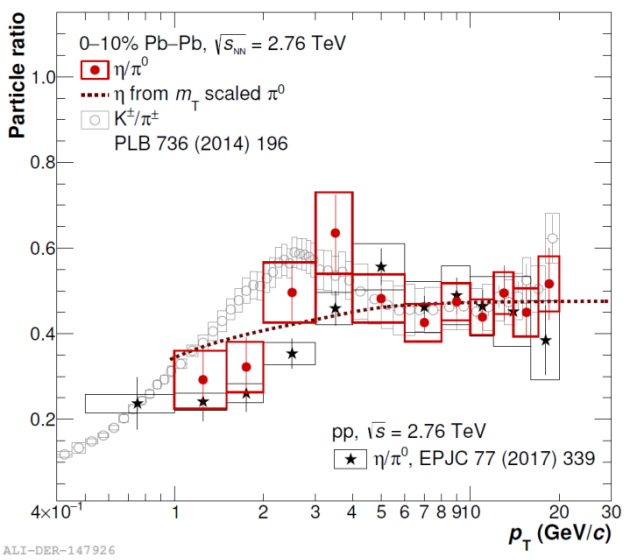

- Constant value of ratio above p_T = 4 GeV/c.
- Comparison of η/π^0 ratio for two centrality classes in Pb-Pb at $\sqrt{s_{NN}}$ = 2.76 TeV to pp result at $\sqrt{s}$ = 7 TeV
  $\Rightarrow$ no significant differences.

- Theory jet quenching predictions by Wei Dai et al. (arXiv:1506.00838) compared to data.
- Good description of ratio within uncertainties.

- Comparison of η/π^0 ratio for two centrality classes to $K^{\pm}/\pi^{\pm}$ ratio measured by ALICE (PLB 736 (2014) 186).
- Consistency of trend and magnitude.

Conversions

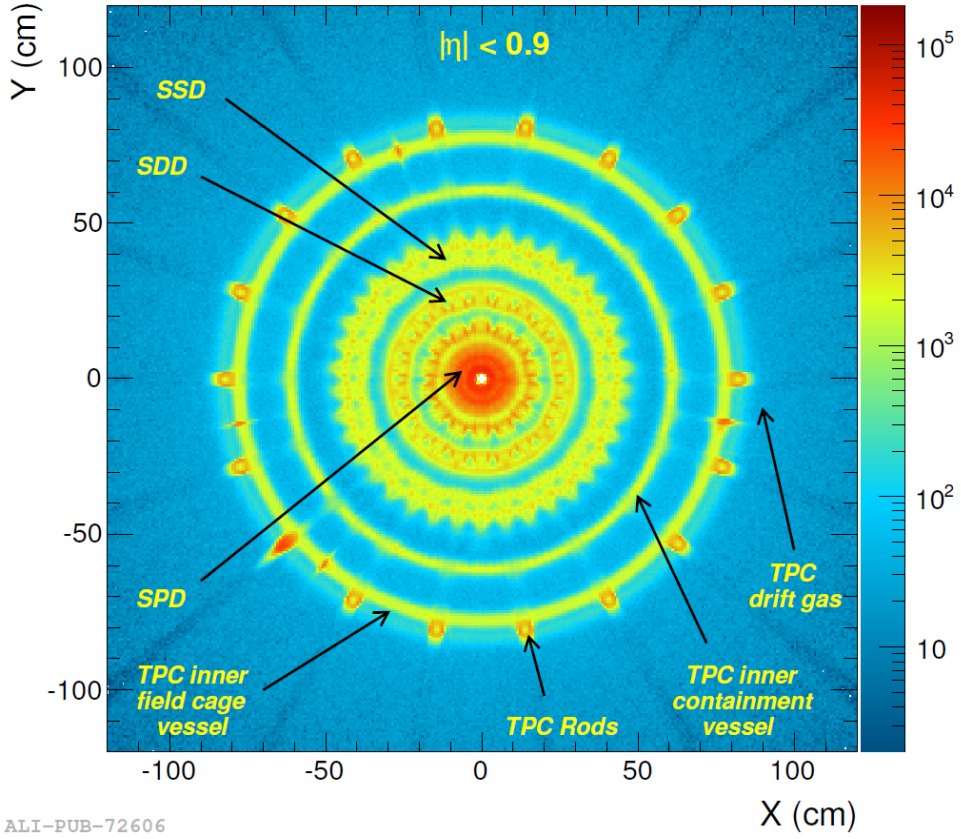

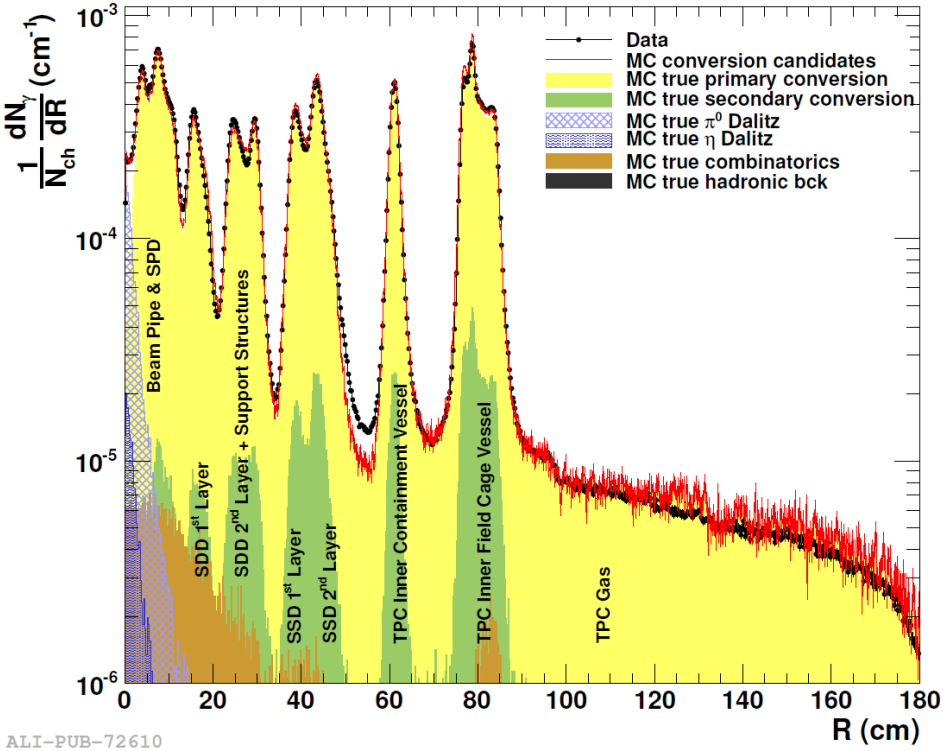

From binary to nuclear collisions

- pp collisions
  - “Vacuum” (no medium)
  - Should be well understood
  - Reference data

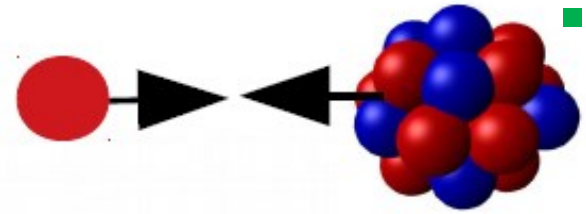

- p-Pb collisions
  - Control experiment
  - Hadronic matter
  - Cold Nuclear Matter effects (related to the difference for a parton being part of a nucleon or a nucleus, e.g. modifications to PDF, Cronin)

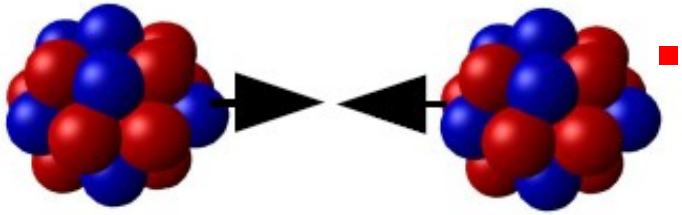

- Pb-Pb collisions
  - Investigate strongly interacting matter at high energy density (QGP)

Large Hadron Collider

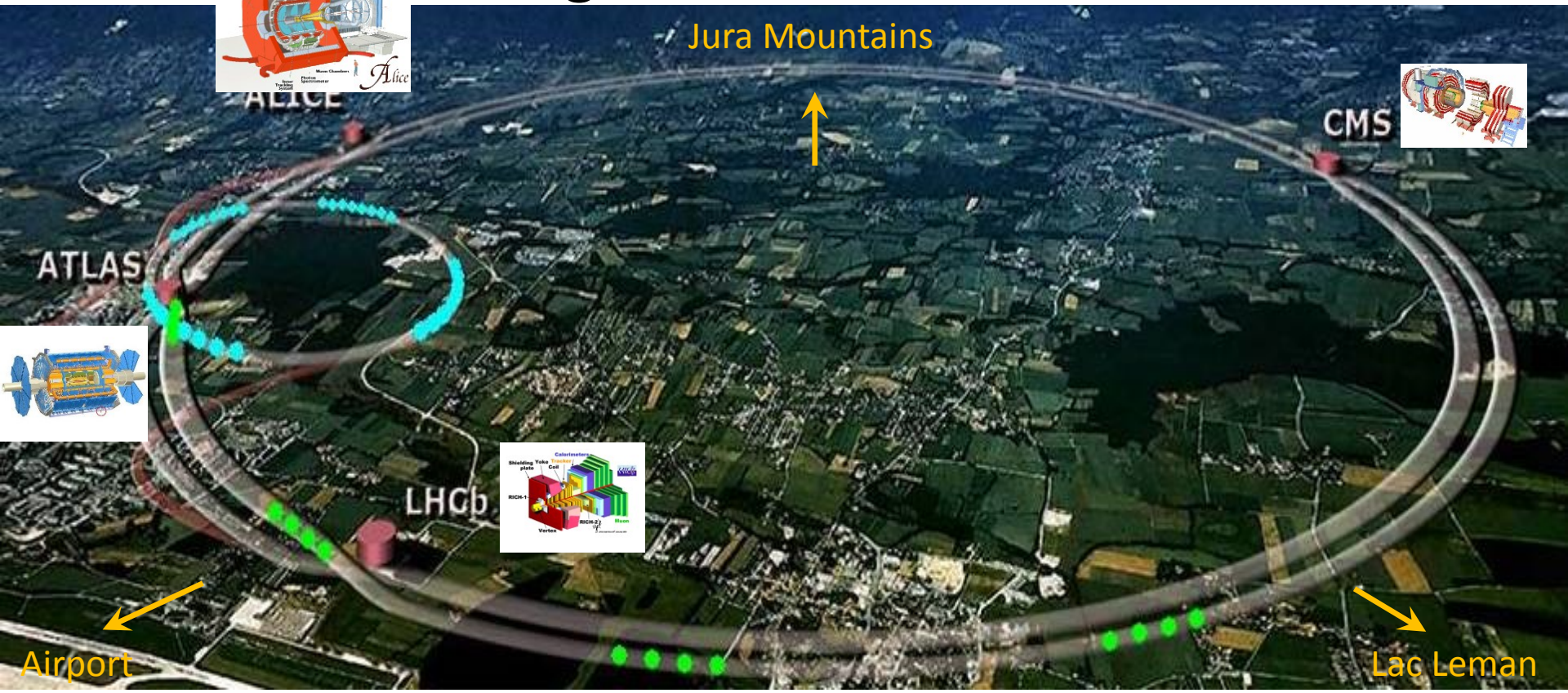

System	Run 1 (2009 - 2013)	Run 2 (2015 - now)
pp	$\sqrt{s}$ = 0.9, 2.76, 7, 8 TeV	$\sqrt{s}$ = 5.02, 13 TeV
p-Pb	$\sqrt{s_{NN}}$ = 5.02 TeV	$\sqrt{s_{NN}}$ = 5.02, 8.16 TeV
Pb-Pb	$\sqrt{s_{NN}}$ = 2.76 TeV	$\sqrt{s_{NN}}$ = 5.02 TeV
Xe-Xe		$\sqrt{s_{NN}}$ = 5.44 TeV

year	$\sqrt{s_{NN}}$ (TeV)	L_{int} (nb^{-1})	year	$\sqrt{s_{NN}}$ (TeV)	L_{int} (nb^{-1})
2010 Pb-Pb	2.76	2.3×10^{-3}	2015 pp	5.02	2.0
2011 pp	2.76	13.8	2015 Pb-Pb	5.02	0.012
2011 Pb-Pb	2.76	0.10	2017 Xe-Xe	5.44	0.19×10^{-3}
2013 p-Pb	5.02	0.05	2017 pp	5.02	18.8
2013 pp	2.76	47.1	(in this analysis)		

Neutral mesons in p-Pb @5.02 TeV

EPJC 78 (2018) 624

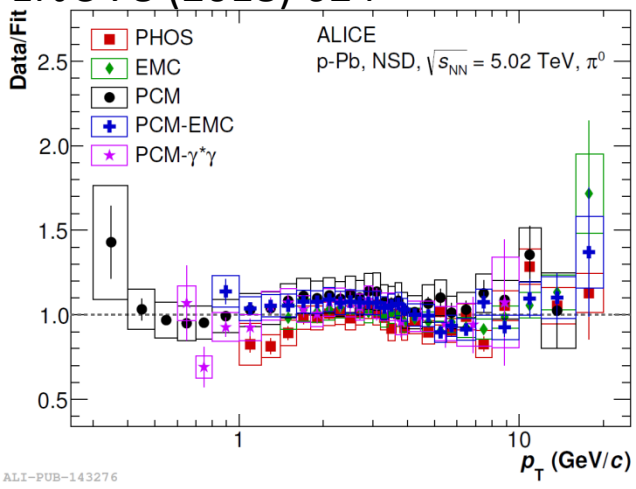

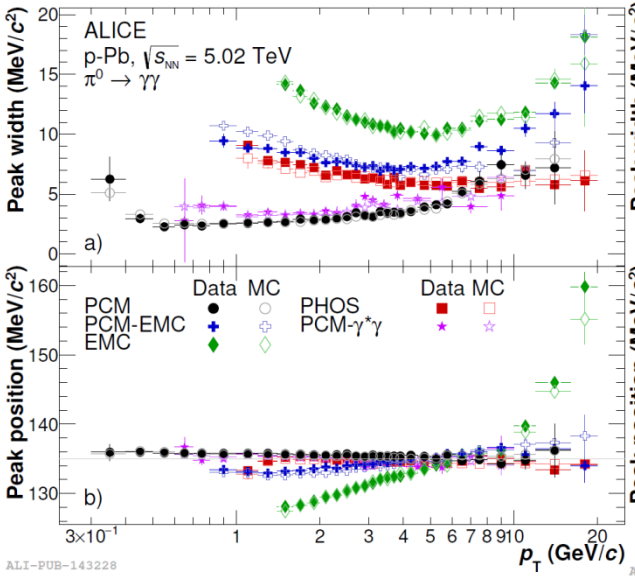

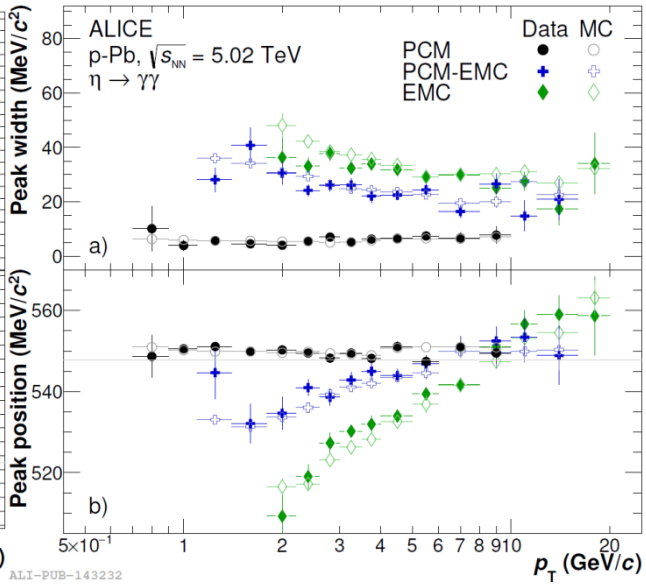

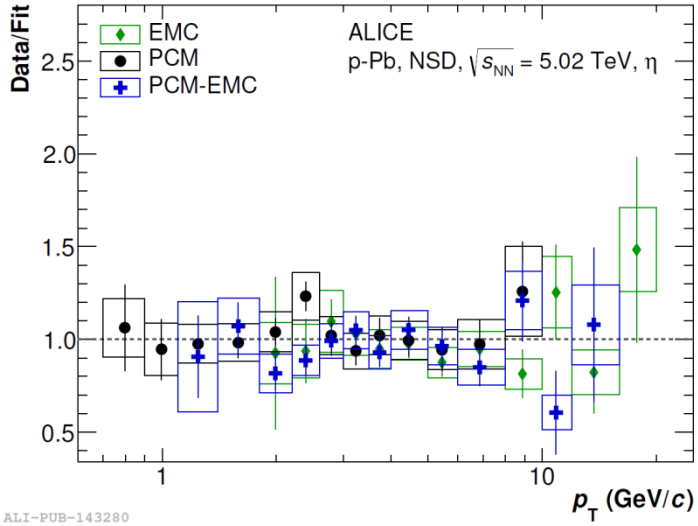

	Relative systematic uncertainty (%)									
	PHOS		EMC		PCM		PCM–$\gamma^*\gamma$		PCM-EMC	
	p_T (GeV/c)		p_T (GeV/c)		p_T (GeV/c)		p_T (GeV/c)		p_T (GeV/c)	
	1.5	7.5	1.5	14.0	1.5	7.5	0.9	3.1	1.5	7.5
Material budget	3.5	3.5	4.2	4.2	9	9	4.5	4.5	5.3	5.3
Yield extraction	2.2	2.5	1.5	3.6	2.2	1.5	3.5	1.1	1.2	2.6
γ reconstruction					0.9	3.0	2.3	1.8	0.6	1.7
e^+/e^- identification					0.8	2.4	2.7	2.3	0.5	0.8
Track reconstruction					0.3	0.7	1.6	2.0	0.5	0.7
Sec. e^+/e^- rejection							4.5	2.8		
Dalitz branching ratio							3.0	3.0		
Cluster energy calib.	4.9	6.2	1.7	2.5					2.0	2.6
Cluster selection			4.6	5.1					1.1	1.7
π^0 reconstruction			0.9	3.9	0.9	1.1	1.9	2.0	0.3	0.3
Secondary correction	2.0	2.0								
Generator efficiency			2.0	2.0					2.0	2.0
Acceptance	2.2	2.2								
Bkg. estimation	4.6	4.9			0.1	0.1	1.8	2.0		
Pile-up correction	1.0	1.0			0.8	0.3				
Total	8.5	9.5	7.0	9.1	9.4	10.0	9.2	7.7	6.3	7.2

Table 3: Relative systematic uncertainties (%) of the π^0 spectrum for the different reconstruction methods.